

1  
2  
3 **Two-dimensional vapour intrusion model involving advective transport of**  
4 **vapours with a highly permeable granular layer in the vadose zone serving**  
5 **as the preferential pathway**  
6  
7

8  
9 Aravind Unnithan<sup>1</sup>, Dawit Nega Bekele<sup>1,4</sup>, Sreenivasulu Chadalavada<sup>1,3</sup>, Ravi Naidu<sup>1,2</sup>  
10

11  
12  
13  
14 <sup>1</sup> Global Centre for Environmental Remediation, The University of Newcastle, University  
15 Drive, Callaghan NSW 2308, Australia  
16

17  
18  
19 <sup>2</sup> CRC CARE, ATC Building, The University of Newcastle, University Drive, Callaghan  
20 NSW 2308, Australia  
21

22  
23  
24 <sup>3</sup> School of Engineering, The University of Southern Queensland, 37 Sinnathamby  
25 Boulevard, University Drive, Springfield Lakes QLD 4300, Australia  
26

27  
28 <sup>4</sup> Douglas Partners Pty Ltd. 439 Montague Road, West End QLD 4101, Australia  
29  
30

31  
32  
33  
34  
35  
36 Corresponding author:

37  
38 Ravi Naidu <sup>1,2</sup>  
39

40  
41 Email address: [Ravi.Naidu@newcastle.edu.au](mailto:Ravi.Naidu@newcastle.edu.au)  
42  
43  
44  
45  
46  
47  
48  
49  
50  
51  
52  
53  
54  
55  
56  
57  
58  
59  
60  
61  
62  
63  
64  
65

## Response to reviews - Ms. Ref. No.: STOTEN-D-22-17016

We are highly indebted to the reviewers for the constructive comments on our manuscript entitled “Two-dimensional chlorinated vapour intrusion model involving advective transport of vapours with a highly permeable granular layer in the vadose zone serving as the preferential pathway”. We have undertaken revision of our manuscript based on the comments and all changes are highlighted in the manuscript. Listed below are actions that we have taken in response to the comments by the reviewers on a point-by-point basis.

**Reviewer #1:** The authors only partially addressed my comments to the first version of the paper. In general, rewriting of the paper was quite limited, the minimum work required to address the issues raised in my review. Instead, the following points still need to be addressed:

Table 3: the choice of total, air filled and water filled porosity and soil air permeability has surely an influence on the results. I suggest to carry out a sensitivity analysis on this parameters so to assess their influence on the calculated indoor air concentration.

Section 3.2: given the comment above, it would be useful to show the results obtained with different permeability and porosities. The authors did not add any kind of the sensitivity analysis, stating that they will be published in another work with reference to a case study. My request was more general, to have more information on the response of the model to different inputs on key parameters, such as water filled porosity and soil permeability.

Author response: I have acknowledged the reviewer’s comment and the manuscript has been revised by including a sensitivity analysis section on page 23 (line 373). The effect of different soil types and change in soil porosity and moisture is discussed in this section.

Section 3.1.1 and 3.1.2: Both these sections deal with the comparison of the developed model with other models. Nevertheless, I do not understand the significance of this comparison. Before, you state that few models address the issue of lateral dispersion but here you assume lateral distance of the building equal to zero. Given my comment above, different models/data are needed for the validation of the new proposed model. For example Feng et al. (JCH, 2020) report an analytical solution of a model for a layered soil laterally away from the edge of the source. The authors did not include any further comparison on this key issue of the proposed model, i.e. how the model simulates lateral dispersion. I still think that further validation is required. For this reason, I ask the authors a further step to improve the paper.

Author response: Thank you for the suggestion. Previously, the lateral distance was considered zero to take into account commonly used CSMs where a building is directly over a contaminant plume. However, to stick to the CSM considered in this study, the model verification is conducted by comparing the results of the normalised sub-slab concentration obtained from the current model with the results of analytical approximation method (AAM)

(Yao et al., 2013) and Abreu and Johnson's 3-D model (Abreu and Johnson, 2005) for different values of source-building lateral separation (page 16; line 267). Further validation of the model is limited due to the lack of published data with highly permeable granular layer as preferential pathway.

1     **Two-dimensional chlorinated vapour intrusion model involving advective**  
2     **transport of vapours with a highly permeable granular layer in the vadose**  
3             **zone serving as the preferential pathway**

4     Aravind Unnithan<sup>1</sup>, Dawit Nega Bekele<sup>1,4</sup>, Sreenivasulu Chadalavada<sup>1,3</sup>, Ravi Naidu<sup>1,2</sup>

5

6     <sup>1</sup> Global Centre for Environmental Remediation, The University of Newcastle, University  
7             Drive, Callaghan NSW 2308, Australia

8     <sup>2</sup> CRC CARE, ATC Building, The University of Newcastle, University Drive, Callaghan  
9             NSW 2308, Australia

10    <sup>3</sup> School of Engineering, The University of Southern Queensland, 37 Sinnathamby Boulevard,  
11             University Drive, Springfield Lakes QLD 4300, Australia

12    <sup>4</sup> Douglas Partners Pty Ltd. 439 Montague Road, West End QLD 4101, Australia

13

14

15    Corresponding author:

16    Ravi Naidu <sup>1,2</sup>

17    Email address: [Ravi.Naidu@newcastle.edu.au](mailto:Ravi.Naidu@newcastle.edu.au)

18 **Abstract**

19 Vapour Intrusion (VI) is the process through which volatile organic compounds migrate from  
20 the subsurface source to the soil predominantly by diffusion, entering the overlying buildings  
21 through joints, cracks or other openings. This activity poses potentially serious health hazards  
22 for the occupants. Because of these health risks, recommendations for site closure are often  
23 made by quantifying the VI risks using mathematical models known as ‘Vapour Intrusion  
24 Models’ (VIM). Most of these VIMs seem to overlook the role of preferred pathways like utility  
25 lines, high conductivity zones of soil or rocks, etc., which act as the path of least resistance for  
26 vapour transport thereby increasing vapour intrusion risks. This study presents a two-  
27 dimensional (2-D) chlorinated vapour intrusion (CVI) model which seeks to estimate the  
28 source-to-indoor air concentration attenuation. It takes into account the effects of a highly  
29 permeable utility line embedment as a preferential pathway. The transport of 2-D soil gas is  
30 described using the finite difference method where advection serves as the dominant transport  
31 mechanism in the preferential pathway layer, while diffusion applies to the rest of the vadose  
32 zone. The model returned results comparable with other models for the same input parameters,  
33 and was found to closely replicate the results of 3-D models. The simulations indicate that the  
34 presence of highly permeable utility line embedment and backfill layers do trigger a higher  
35 indoor air concentration compared to a no preferential pathway scenario.

36 **Keywords:** Vapour intrusion; two dimensional model; preferential pathway; chlorinated  
37 hydrocarbons.

38 **Funding**

39 This research did not receive any specific grant from funding agencies in the public,  
40 commercial, or not-for-profit sectors.

41

## 42        **1. Introduction**

43        The conceptual site models (CSMs) help in identifying the pathways for vapour transport in the  
44        vadose zone and its entry into buildings. Conventional CSMs assume a ‘soil VI pathway’ in  
45        which vapours from a subsurface source emanate and diffuse vertically and/or laterally through  
46        the subsurface soil, which then intrudes into the indoor air typically through foundation pores,  
47        cracks or openings (Guo et al., 2015). However, the presence of alternate exposure pathways  
48        in the vadose zone like utility lines, naturally occurring fractures or macro pores, highly  
49        permeable soil layers or backfills etc. had been generally overlooked until recently. These  
50        alternative exposure pathways, known as preferential pathways, intersect with the vapour  
51        source or vapour migration pathways offer least resistance to soil vapour flow, subsequently  
52        and significantly increasing the risk of vapour intrusion (VI) (USEPA, 2002). The majority of  
53        vapour intrusion models (VIMs) currently in use have been developed with conventional CSMs  
54        but have often ignored the potential for vapour entry into indoor air scenarios through utility  
55        corridors, plumbing systems, etc., during VI investigations and developing VIMs. Failure to  
56        incorporate the role of preferential pathways into VI results in inaccurate predictions of indoor  
57        air vapour concentrations and wrong clean-up strategies.

58        The United States Environmental Protection Agency (US EPA) recommended a buffer zone of  
59        about 100 feet (or 30 m) vertically and laterally from the contaminant source, beyond which  
60        buildings can be deemed safe since no significant indoor air concentration had been found in  
61        them at a distance greater than one house lot (USEPA, 2002). Yet, in recent studies, VI impacts  
62        were detected in buildings even outside the footprint of the contaminant plume (Yao et al.,  
63        2017a) due to the presence of preferential pathways which offer little vapour attenuation and  
64        this leads to high indoor air concentrations. Most of the VI through preferential pathways are  
65        related to the interception of compromised or deteriorated sewer systems, primarily designed  
66        to carry wastewater to treatment plants, with the contaminant plume in vadose zone ultimately  
67        resulting in unhindered transport of volatile organic compounds (VOCs) into the indoor air

68 through connected plumbing systems (Jacobs et al., 2015). Several field studies have been  
69 conducted in recent times confirming the role of sewers acting as a preferential pathway for soil  
70 vapour transport, resulting in significant indoor air contaminant concentrations even in  
71 buildings outside the groundwater plume area (Distler and Mazierski, 2010, Riis et al., 2010,  
72 Vroblesky et al., 2011, Pennell et al., 2013, Guo et al., 2015, McHugh et al., 2017, Guo et al.,  
73 2020, Beckley and McHugh, 2021). Additionally, VI episodes without a vadose zone source  
74 can occur from VOCs volatilising from industrial discharges which are directly discharged into  
75 sewer systems which contribute to higher indoor air contaminant concentrations (Roghani et  
76 al., 2018).

77 Many studies conducted on preferential pathways in VI focus on contaminant transport through  
78 sewers, utility tunnels and their associated plumbing conduits. However, the role of highly  
79 permeable soil layers and backfill materials in VI have rarely been investigated. The presence  
80 of any high permeability region in the vadose zone - either natural or anthropogenic - can  
81 function as a preferential pathway in contaminant vapour transport. These regions of high  
82 permeability can occur naturally as gravel layers or fractured rocks which facilitate higher  
83 contaminant flux owing to their higher porosity (USEPA, 2015b). As well, granular fill  
84 materials laid as bedding and embedment to utility lines can cause high contaminant flux  
85 laterally and vertically to the ground surface, and thereby serve as preferential pathways (ITRC,  
86 2014).

87 The aim of this study is to develop and evaluate a 2-D model in order to estimate the indoor air  
88 concentration at sites contaminated with chlorinated hydrocarbons (CHCs) with a highly  
89 permeable gravel layer acting as a preferential pathway. The numerical model depicts: i) two-  
90 dimensional vapour flux (lateral and vertical directions) of chlorinated hydrocarbon  
91 contaminants; ii) the building of concern laterally situated at a distance from the edge of the  
92 contaminant plume; and iii) the presence of a highly permeable coarse grained soil layer such  
93 as gravel used as bedding for utility lines which act as preferential pathway for vapour transport.

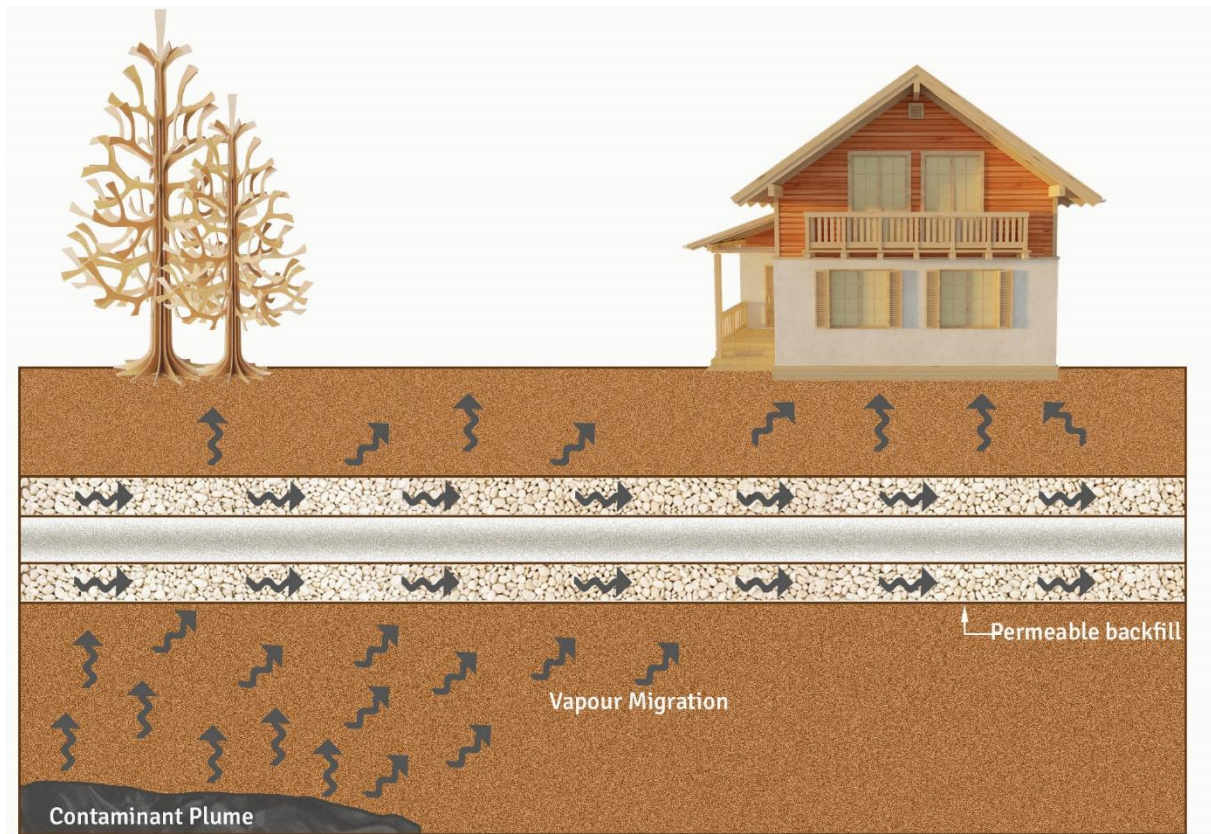


94 This model: firstly, solves partial differential equations of diffusion and advection in the vadose  
95 zone with preferential pathway to estimate the total vapour flux; secondly, has a modular  
96 subroutine for simulating the effect of preferential pathway in vapour transport; and thirdly,  
97 estimates the indoor air concentration by ‘continuous stirred tank reactor method’ as employed  
98 in Johnson and Ettinger’s (hereafter J&E) model. Evaluating the model’s performance was  
99 carried out by comparing it with 1-D, 2-D and 3-D models using hypothetical as well as field  
100 data obtained from particular studies (Holton et al., 2013, Guo et al., 2015, Yao et al., 2017b).

## 101 **2. Methodology**

### 102 **2.1. Model development**

103 The numerical model took two stages to develop. First, a conceptual model was devised  
104 considering: i) the system as two-dimensional; ii) the building of concern placed laterally at a  
105 distance from the edge of the CHC contaminant plume; iii) a coarse grained utility line bedding,  
106 such as gravel, sand or crushed stone with high permeability acting as the path of least resistance  
107 for the contaminant vapour flux; and iv) foundation of the building as slab-on-grade and  
108 simulating the interaction between the sub-surface and the building. The purpose of this  
109 conceptual model is to illustrate the role of highly permeable bedding layers of utility lines in  
110 exacerbating the risk of VI in buildings located laterally at a distance from the edge of the  
111 contaminant plume. The general CSM developed for this study is depicted in Figure 1.



112

113

Figure 1. CSM developed for the study

114

In the second stage of model’s development, governing equations were formulated and solved

115

using the central difference scheme of the finite difference method and coded in Python

116

programming language for simulating fate and transport of CHCs from source to the building

117

foundations through sub-surface soil. The vapour entry into the building through the

118

foundations and subsequent indoor air contaminant concentration is calculated using the

119

‘continuous stirred tank reactor method’ employed in the J&E model (Johnson and Ettinger,

120

1991).

121

Although there are several models which consider two-dimensional vapour transport, most of

122

them assume diffusion is the dominant transport mechanism in the vadose zone but do not take

123

into account the presence of a preferential pathway. Some guidance documents suggest the role

124

of natural and induced high permeability zones in the vadose zone as preferential pathways, for

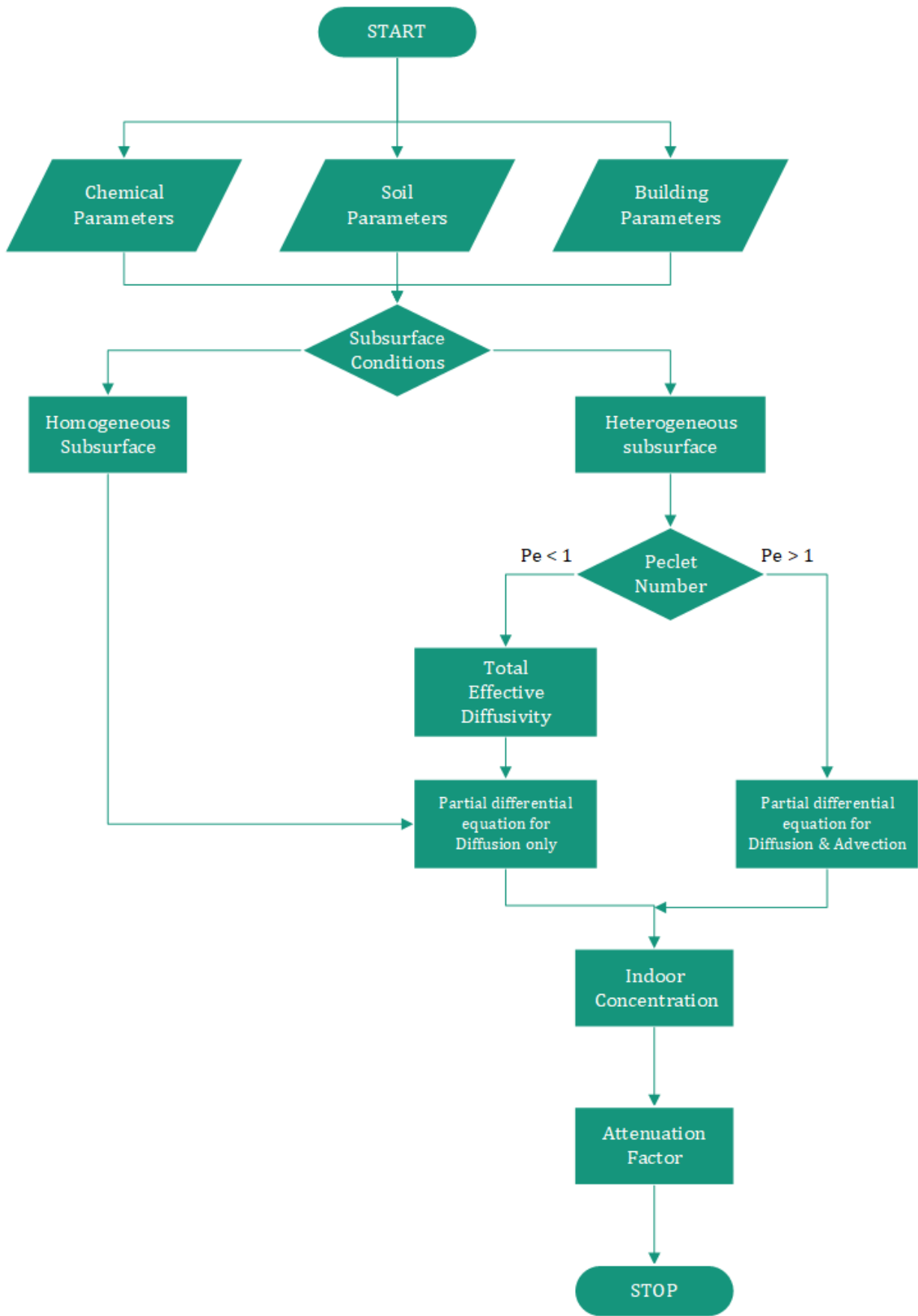
125

instance gravel and sand lenses, vertically fractures rocks, etc., as well as highly permeable

126

bedding or backfill layers of utility lines which are mostly situated close to the surface (USEPA,

127 2015a, ITRC, 2014). However, we know of few studies that have shown vapour migration  
128 through backfills or naturally occurring high permeability zones which this model seeks to  
129 address. When a significant pressure gradient is present, an upward advective soil gas transport  
130 might be induced which can be identified using Peclet number ( $Pe$ ) (Yao et al., 2015). If  $Pe > 1$ ,  
131 it is assumed that advection will be the dominant transport mechanism but it will be diffusion  
132 if  $Pe < 1$ . The flowchart shown in Figure 2 illustrates the steps involved in developing the 2-D  
133 model for simulation of CHC vapour transport in the presence of a highly permeable  
134 preferential pathway layer. This model calculates the indoor air concentration and attenuation  
135 factor by simulating the vapour transport in the vadose zone. It does this by considering  
136 diffusion as the dominant transport mechanism if  $Pe < 1$  and advection as the dominant transport  
137 mechanism if  $Pe > 1$  in the bedding and backfill layer.



138

139

Figure 2: Overview of the 2-D model process with the preferential pathway

140 The major components involved in the model's methodology are: i) obtaining the vapour flux  
141 and contaminant concentration profile in the vadose zone; ii) determining the dominant  
142 transport mechanism in the backfill and bedding layer by computing  $P_e$ ; iii) calculating vapour  
143 entry into the building using continuous stirred tank reactor method; and iv) computing indoor  
144 air concentration and attenuation factor based on the subsoil and building interaction. The effect  
145 of preferential pathways in three scenarios considered in this study are: i) preferential pathway  
146 closer to the source; ii) preferential pathway equidistant from the source and receptor; and iii)  
147 preferential pathway furthest from the source. Results of these simulations are then compared  
148 with a 'no-preferential pathway' scenario in order to fully understand the role of the highly  
149 permeable bedding layer in exacerbating the VI risk.

150 For refining the numerical model, the following assumptions are made. Firstly, the model  
151 operates under steady state conditions. The source concentration is considered to be constant  
152 and the vapour migration is deemed to be a steady-state process. Although the actual vapour  
153 migration is a transient process, the steady state scenario can express the most hazardous  
154 scenario. Secondly, the subsurface is assumed to be stratified due to the presence of the  
155 preferential pathway and each soil layer is homogeneous. Thirdly, the contaminant  
156 concentration decreases exponentially with lateral distance from the source. Fourthly, the utility  
157 line is leak-proof and does not act as preferential pathway. Fifthly, the effect of biodegradation  
158 is not taken into account since the rate of degradation of TCE is negligible without a growth  
159 substrate like methane (Choi et al., 2002). The vapour concentrations and subsequent indoor air  
160 concentration calculated under these assumptions can be overestimated compared to actual on-  
161 site measurement. Nevertheless, the model can be employed as a screening tool to address the  
162 VI problem with a preferential pathway.

## 163 **2.2. Governing equations and boundary conditions**

### 164 **2.2.1. Transport by diffusion**

165 The vapour transport in the vadose zone is assumed to be steady state diffusion except in the  
 166 highly permeable preferential pathway layer. Since both lateral and vertical movement of the  
 167 contaminant vapours are considered in a two-dimensional soil context, the governing equation  
 168 for the transport of a non-reacting, non-adsorbing vapour through the vadose zone under steady  
 169 state diffusion is explained by Laplace equation as given in eq. (1) (Yao et al., 2017b):

$$170 \left( \frac{\partial^2 C}{\partial x^2} + \frac{\partial^2 C}{\partial y^2} \right) = 0 \quad (1)$$

171 where:  $x$  and  $y$  are lateral and vertical coordinates (m), respectively; and  $C$  denotes the  
 172 contaminant vapour concentration (mg/L).

173 The effective vapour diffusion coefficient of the media,  $D_e$  ( $m^2/s$ ), is calculated using the  
 174 Millington-Quirk equation (1961) as given in eq. (2):

$$175 D_e = D_a \frac{\theta_a^{10/3}}{\theta_T^2} + \frac{D_w \theta_w^{10/3}}{H \theta_T^2} \quad (2)$$

176 where:  $D_a$  is the molecular diffusion coefficient in gas ( $m^2/s$ );  $D_w$  stands for the molecular  
 177 diffusion coefficient in water ( $m^2/s$ );  $\theta_T$ ,  $\theta_a$  &  $\theta_w$  are total porosity, air filled porosity and water  
 178 filled porosity, respectively; and  $H$  is the dimensionless Henry's law constant.

179 In a heterogeneous subsurface with  $n$  layers of soil, a total effective diffusion coefficient can be  
 180 introduced ( $D_{e,tot}$ ) as shown in eq. (3) which transforms the diffusion coefficients of individual  
 181 soil layers of the subsurface into an equivalent homogeneous system (Johnson and Ettinger,  
 182 1991):

$$183 D_{e(tot)} = \frac{L}{\sum_{i=0}^n \frac{d_i}{D_{e(i)}}} \quad (3)$$

184 where:  $L$  is the depth of vadose zone (m);  $d_i$  is the thickness of the  $i$ th layer (m); and  $D_{e(i)}$   
 185 denotes the effective diffusion coefficient of the  $i$ th layer ( $m^2/s$ ).

186

### 187 2.2.2. Transport by advection

188 In preferential subsurface pathways such as utility corridors, highly permeable soils or porous  
189 zones of rocks, the contaminant vapours tend to migrate via advection (USEPA, 2015a). A  
190 relatively small change in partial pressure can trigger significant advective vapour transport  
191 which is larger than the diffusive fluxes (Scanlon et al., 2002). The contaminant vapours reach  
192 the highly permeable granular fill in the vadose zone from the source. Meanwhile the pressure  
193 difference between the subsurface and open ground and the high soil permeability causes a  
194 change in vapour velocity. This can be calculated using eq. (4) as written below:

$$195 \mathbf{u}_g = \frac{K_{bf}}{\mu} \cdot \nabla P_w \quad (4)$$

196 where:  $u_g$  is the average vapour phase velocity (m/s);  $K_{bf}$  is the soil air permeability of the  
197 granular backfill ( $m^2$ );  $\mu$  stands for soil gas viscosity (Pa.s); and  $\nabla P_w$  represents the vapour  
198 pressure gradient in the granular backfill (Pa), which is required as an independent input of the  
199 model.

200 Once the vapour velocity is obtained, the Peclet number can be computed using eq. (5) to  
201 confirm the dominant transport mechanism in the preferential pathway:

$$202 P_e = \frac{u_g \cdot L}{D_{TCE}} \quad (5)$$

203 where:  $u_g$  is the vapour velocity (m/s);  $L$  is the depth of preferential pathway layer (m); and  
204  $D_{TCE}$  is the effective diffusivity of TCE in soil ( $m^2/s$ ).

205 If  $Pe < 1$ , the dominant transport mechanism will be diffusion and the governing equation is  
206 given by eq. (1). If  $Pe > 1$ , the dominant transport mechanism will be advection for which the  
207 governing equation is given by eq. (6) as stated below:

$$208 -\mathbf{u}_g \left( \frac{\partial C}{\partial x} + \frac{\partial C}{\partial y} \right) = \mathbf{0} \quad (6)$$

209 For geological systems with permeability  $> 10^{-9} \text{ m}^2$ , the contaminant transport can be simulated  
210 with advection equation (Yao et al., 2012).

### 211 **2.2.3. Computation of indoor air concentration**

212 The average indoor air concentration is calculated in this model using the ‘continuous stirred  
213 tank reactor’ method as employed in the J&E model. As per the technical VI guidance of US  
214 EPA (2015a), for a building laterally at a distance from the contaminant plume, the soil vapour  
215 concentration obtained from below the foundation closest to the source can help to describe the  
216 worst case scenario underneath the building. Hence the subslab concentration of vapours  
217  $C(x_{ck}, d_s)$  closest to the edge of the contaminant plume is obtained from the simulations and is  
218 employed for the vapour entry and indoor air concentration calculations using eq. (7) to (14).  
219 The sub-slab crack concentration ( $C_{ck}$ ) can be computed using eq. (7) as documented below:

$$220 \quad C_{ck} = \frac{\pi D_e \cdot d_s \cdot t_{ck}}{D_a w_{ck}} C(x_{ck}, d_s) \quad (7)$$

221 where:  $t_{ck}$  is the thickness of the foundation (m);  $w_{ck}$  is the width of the crack (m);  $x_{ck}$  is the  
222 distance of the foundation crack from the edge of contaminant plume and  $d_s$  is the depth of  
223 source from the foundation.

224 The indoor air contaminant concentration ( $C_{in}$ ) can be calculated as a function of sub-slab crack  
225 concentration as given in eq. (8) using a series of empirical equations as stated in eq. (9) to eq.  
226 (14):

$$227 \quad C_{in} = C_{ck} \left( \frac{R_{mix}}{R_{crack} + R_{mix}} \right) \quad (8)$$

228 Where,

$$229 \quad R_{mix} = \frac{1}{L_{mix} \cdot ER} \quad (9)$$

230 and



$$231 \quad R_{crack} = \left( R_{mix} - \frac{A_b}{Q_s} \right) (e^{-\varepsilon} - 1) \quad (10)$$

232 with

$$233 \quad \varepsilon = \frac{Q_s}{A_b} \frac{t_{ck}}{D_a \eta} \quad (11)$$

$$234 \quad \eta = \frac{w_{ck} l_{ck}}{A_b} \quad (12)$$

$$235 \quad Q_s = \frac{2\pi K_a \Delta p l_{ck}}{\mu \ln\left(\frac{2d_f}{r_{ck}}\right)} \quad (13)$$

236 and

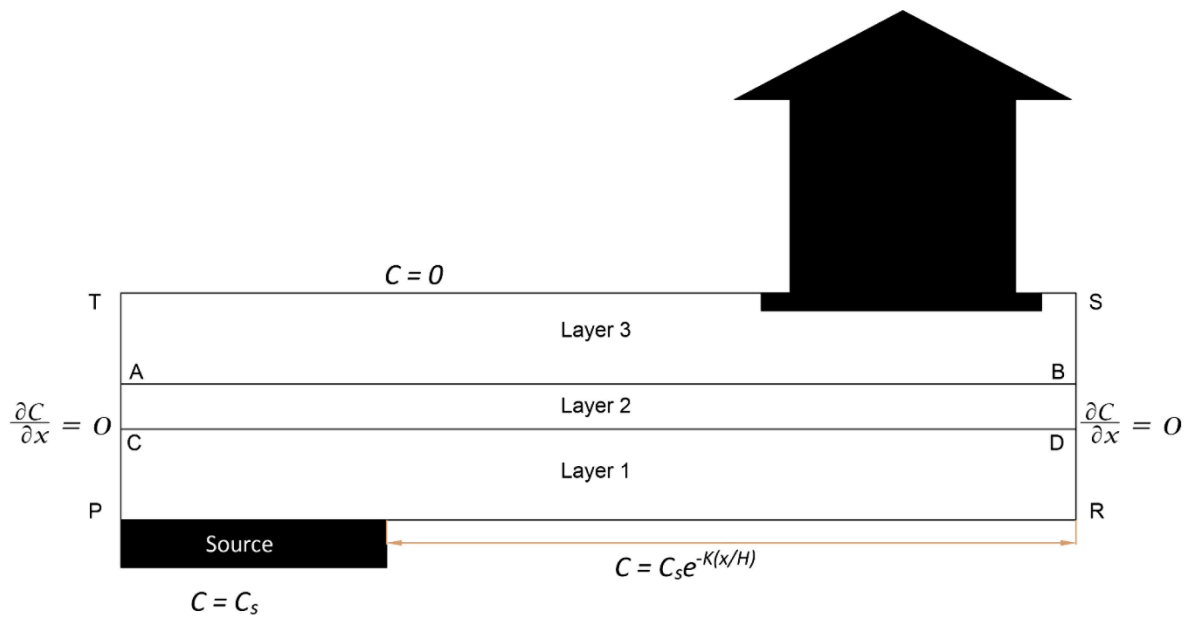
$$237 \quad r_{ck} = \frac{\eta A_b}{l_{ck}} \quad (14)$$

238 where:  $L_{mix}$  (m) denotes the height of the building at which contaminant mixing occurs; ER  
 239 (1/hr) is the building air exchange rate;  $A_b$  ( $m^2$ ) stands for the foundation area in contact with  
 240 the soil;  $Q_s$  ( $m^3/s$ ) is the convective soil vapour entry rate into the building;  $d_f$  (m) is the depth  
 241 of foundation below ground surface;  $\eta$  represents the foundation crack fraction;  $l_{ck}$  (m) is the  
 242 foundation perimeter;  $K_a$  ( $m^2$ ) is the soil air permeability;  $\mu$  (Pa.s) is the soil gas viscosity; and  
 243  $\Delta p$  (Pa) is the pressure difference between building and soil.

244 The sub-slab-to-indoor air concentration attenuation factor ( $\alpha$ ), which relates indoor air vapour  
 245 concentration ( $C_{in}$ ) to the source vapour concentration ( $C_s$ ) can be calculated using eq. (15):

$$246 \quad \alpha = \frac{C_{in}}{C_s} \quad (15)$$

#### 247 **2.2.4. Boundary conditions**



248

$$C = C_s$$

249

Figure 3. Boundary conditions employed for the CSM

250 Figure 3 depicts the boundary conditions for the solution of the transport equations in the vadose

251 zone. The conceptual model assumes concentration at source to be  $C_s$  while the concentration

252 at ground surface is zero. The left-hand and right-hand side boundaries of the domain are

253 assumed to have no flux boundary condition, i.e.  $\frac{\partial C}{\partial x} = 0$  where concentration attenuation is

254 linear. Beyond the edge of the source, the concentration tends towards zero at large lateral

255 distances and the concentration attenuation is exponential which is satisfied by  $C_s e^{-K(\frac{x}{H})}$ ,

256 where:  $x$  is the lateral distance from source (m);  $H$  is the depth of source (m); and  $K$  is the decay

257 rate constant.

258 Boundary condition for advection process in the highly permeable preferential pathway is

259 established by considering the system as three separate layers. The values obtained by solving

260 eq. (1) in layer 1 with the corresponding boundary conditions becomes the boundary condition

261 for layer 2 (CD in fig.3). With  $\nabla P_w$  as independent input in the model, the calculated soil vapour

262 velocity ( $u_g$ ) will determine  $Pe$  which in turn determines the vapour transport mechanism in

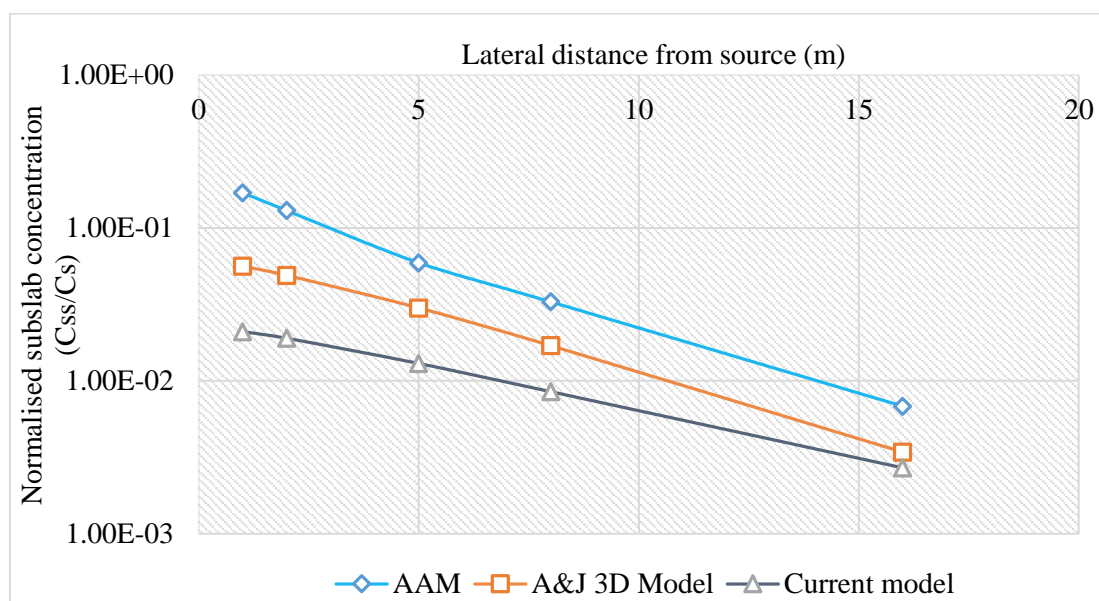
263 layer 2. If  $Pe > 1$ , the transport mechanism will be advection and the system will solve for eq.

264 (6) for the whole layer (until AB in fig. 3). This in turn will serve as the boundary condition for  
265 layer 3 which will solve for diffusion equation for that layer.

### 266 3. Results and Discussion

#### 267 3.1. Comparison with existing models

268 The capability of VI assessment by the developed model is conducted by comparing the results  
269 of the normalised sub-slab concentration obtained from the current model with the results of  
270 analytical approximation method (AAM) (Yao et al., 2013) and Abreu and Johnson's 3-D  
271 model (Abreu and Johnson, 2005). The calculated vapour concentration at the near edge of the  
272 foundation bottom is regarded as the sub-slab concentration. The data adopted for model  
273 comparison is obtained from Yao et al., (2013) for a building foundation depth of 0.2 m and  
274 source depth 8 m for different values of source-building separation. The results of the three  
275 methods are compared in figure 4. With respect to the change in contaminant sub-slab  
276 concentration in lateral direction, the developed model follows the trend of other models,  
277 particularly when compared with the 3-D model, which implies that the developed model may  
278 provide an alternative method of assessing VI risk.



279  
280 Figure 4. The plot of normalised sub-slab concentration ( $C_{ss}/C_s$ ) vs Lateral distance from the  
281 edge of the source for AAM, 3-DM and current model.

282 **3.2.Simulated scenarios**

283 **3.2.1. Effect of preferential pathway**

284 To understand the effect of highly permeable granular fill in the vadose zone in exacerbating  
 285 VI risks, a scenario is simulated by using a granular backfill comprising well graded gravel that  
 286 is 0.5 m in depth. It functions as the preferential pathway at a depth of 1 m from the ground  
 287 surface, where the primary transport mechanism is advection. The building of concern has its  
 288 closest point from the edge of the contaminant plume of concentration 1 g/m<sup>3</sup> at an arbitrarily  
 289 chosen distance of 3 m. The rest of the vadose zone other than the preferential pathway is  
 290 assumed to consist of sandy clay where diffusion is assumed to be the primary transport  
 291 mechanism. The specifications related to pipe embedment and backfilling is consistent with  
 292 Standard drawings SCP-1000 and SCP-1001 of the Standard Technical Specifications for  
 293 Construction of Sewer Rising Mains by Hunter Water Corporation (2005).This is then  
 294 compared to a ‘no-preferential pathway’ scenario where the vadose zone is considered  
 295 homogeneous with sandy clay soil where diffusion is the only soil transport mechanism.  
 296 Biodegradation is not accounted for in the simulations since the contaminant of interest is TCE  
 297 which is normally difficult to biodegrade in soil. The input parameters used in the simulations  
 298 are reported in Table 1.

299 Table 1. Input parameters for the model simulations.

<i>Chemical Parameters</i>		<i>Unit</i>	<i>Value</i>
<i>Source vapour concentration</i>	C <sub>s</sub>	g/m <sup>3</sup>	1
<i>Diffusion coefficient in air</i>	D <sub>a</sub>	m <sup>2</sup> /s	7.90E-06
<i>Diffusion coefficient in water</i>	D <sub>w</sub>	m <sup>2</sup> /s	9.10E-10
<i>Henry’s law constant</i>	H	-	0.403
<i>Soil gas viscosity</i>	μ	Pa.s	5.32E-04
<b><i>Soil Parameters</i></b>			
<i>Total Porosity</i>	Θ <sub>T</sub>	-	0.385
<i>Air filled porosity</i>	Θ <sub>a</sub>	-	0.188
<i>Water filled porosity</i>	Θ <sub>w</sub>	-	0.197
<i>Soil air permeability</i>	K <sub>a</sub>	m <sup>2</sup>	1.70E-13
<b><i>Granular backfill soil parameters</i></b>			

<i>Depth of backfill</i>	ds	m	0.5
<i>Total Porosity</i>	$\Theta_T$	-	0.5
<i>Air filled porosity</i>	$\Theta_a$	-	0.49
<i>Water filled porosity</i>	$\Theta_w$	-	0.01
<i>Soil air permeability</i>	$K_a$	m <sup>2</sup>	1.00E-09
<b><i>Building parameters</i></b>			
<i>Width of foundation slab</i>		m	10
<i>Foundation footprint area</i>	$A_b$	m <sup>2</sup>	100
<i>Depth of foundation below grade</i>	$d_f$	m	0.3
<i>Thickness of foundation crack</i>	$t_{ck}$	m	0.1
<i>Width of foundation crack</i>	$w_{ck}$	m	0.001
<i>Foundation perimeter</i>	$l_{ck}$	m	40
<i>Building height</i>	$L_{mix}$	m	3
<i>Building Air exchange rate</i>	ER	h <sup>-1</sup>	0.5
<i>Soil and building pressure difference</i>	$\Delta p$	Pa	5

300

301 From the simulations, it was observed that there was a considerable increase, virtually double  
302 the amount, in sub-slab as well as indoor air concentrations in the presence of a highly  
303 permeable preferential pathway layer when compared to the ‘no-preferential pathway’ scenario.  
304 Table 2 shows the contrasts in vapour concentration in the sub-slab and indoor air and the  
305 attenuation factor with and without the preferential pathway. Based on these results, it is clearly  
306 evident that the presence of preferential pathway indeed increases the potential risk of VI.

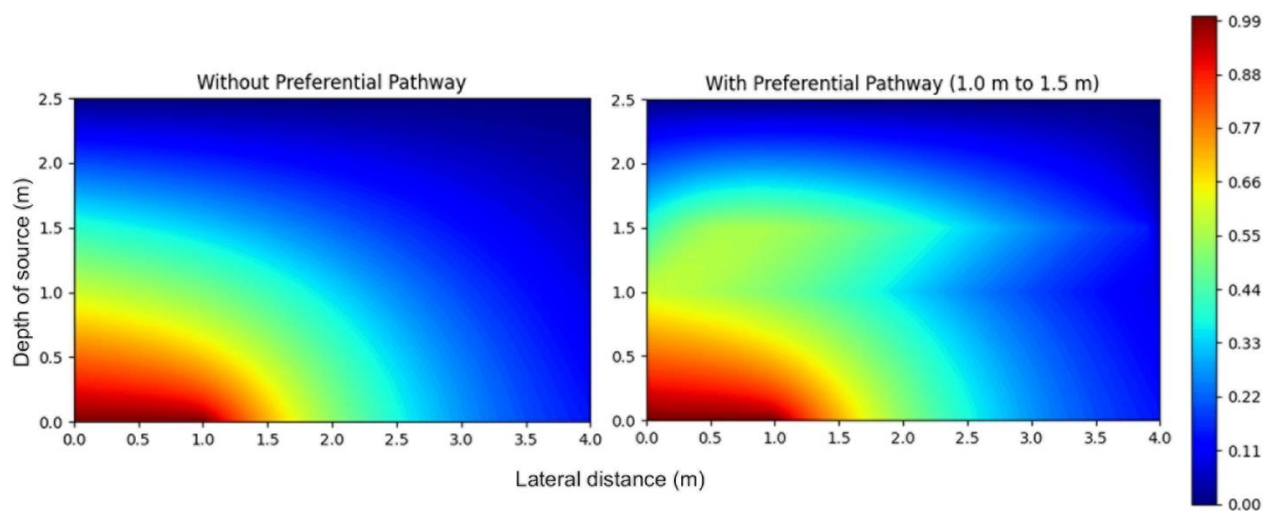
307 Table 2. Comparison of sub-slab concentration, indoor air concentration and attenuation factor  
308 with and without the preferential pathway for different scenarios.

	<i>Without preferential pathway</i>	<i>With preferential pathway</i>
<i>Source concentration (g/m<sup>3</sup>)</i>	1	1
<i>Sub-slab concentration (g/m<sup>3</sup>)</i>	0.025	0.048
<i>Indoor air concentration (g/m<sup>3</sup>)</i>	3.86E-05	7.40E-05
<i>Attenuation factor (<math>\alpha</math>)</i>	3.86E-05	7.40E-05

309

310 This increase in indoor air contaminant concentration can be attributed to the limited attenuation  
311 occurring in the preferential pathway. Advection is assumed to be the dominant transport  
312 mechanism in the preferential pathway layer, so the vapour movement occurs at a faster rate.

313 This is comparable to the rest of the vadose zone where vapour transport occurs due to diffusion,  
314 hence offering the least resistance for soil gas transport and subsequently less attenuation.  
315 Figure 5 presents the vapour concentration profile in the vadose zone which shows the increase  
316 in vapour concentration in the preferential pathway layer as opposed to that of a ‘no-preferential  
317 pathway’ scenario. It proves that the preferential pathway offers the least resistance to vapour  
318 transport in the vadose zone and ultimately results in exacerbation of VI.

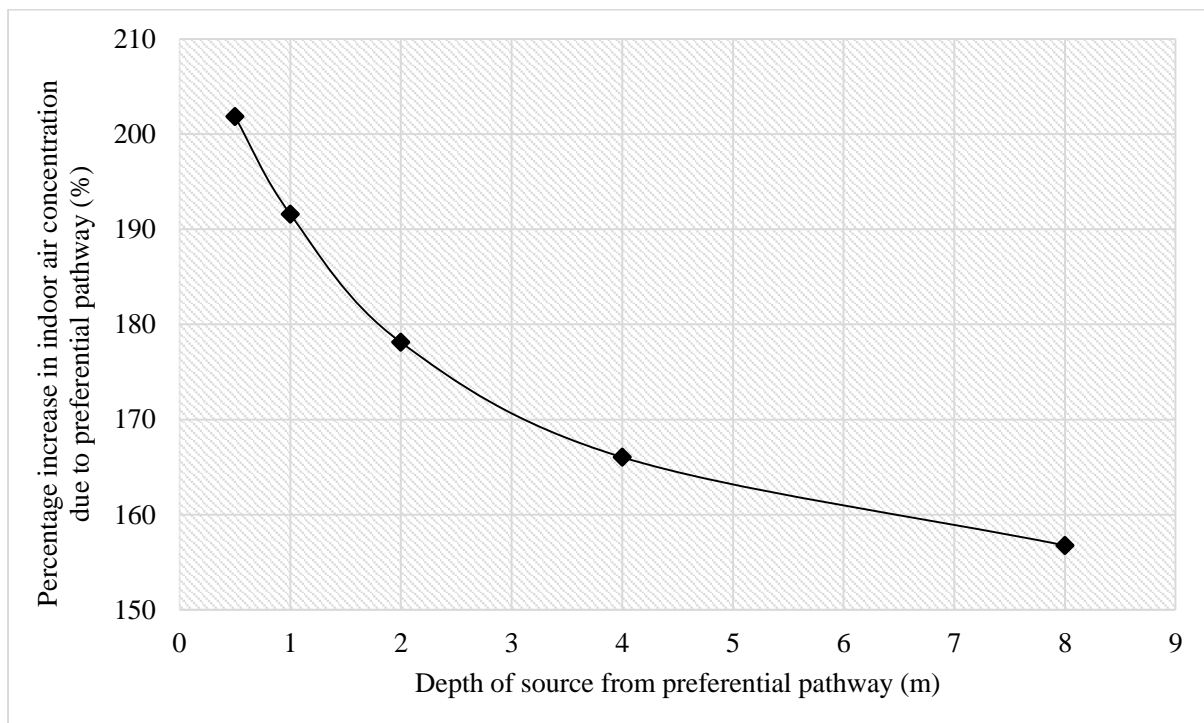


319  
320 Fig. 5: Comparison of vapour concentration profile in the vadose zone with and without the  
321 preferential pathway for the same scenario.

### 322 3.2.2. Influence of depth of source from preferential pathway

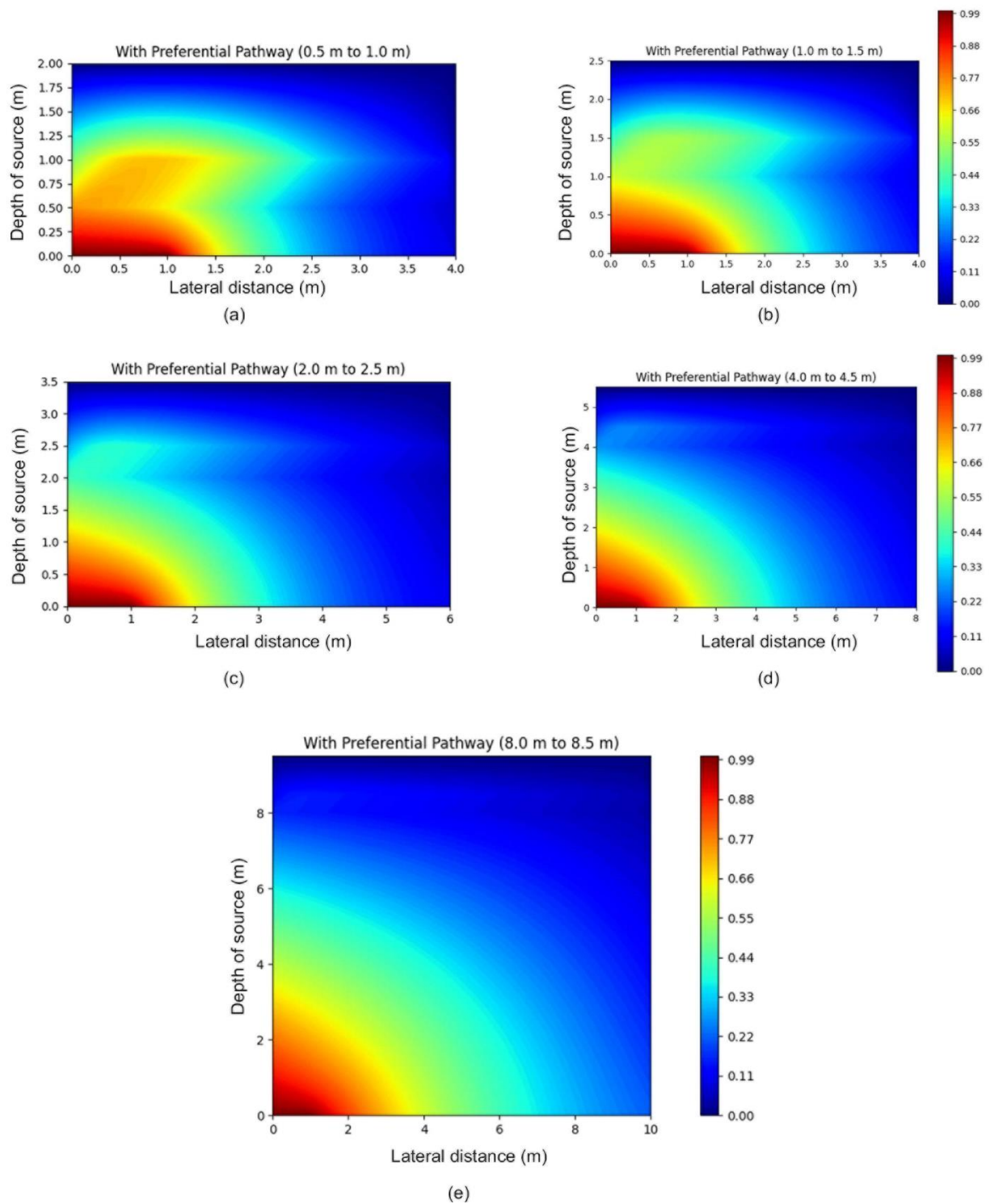
323 Simulations were conducted to understand the effect of proximity of the source to the  
324 preferential pathway by varying the depth of source (0.5 m, 1 m, 2 m, 4 m & 8 m) from the  
325 preferential pathway, retaining the remainder of the vadose zone conditions and the input  
326 parameters the same as that of the previous simulation. The closer the source is to the  
327 preferential pathway, the distance of vapour transport in soil before reaching the preferential  
328 pathway diminishes, resulting in less vapour attenuation. This causes a high vapour  
329 concentration to enter the preferential pathway which then travels with comparatively least  
330 resistance till the upper layer of soil with lesser attenuation, leading to an increase in indoor air  
331 concentration. Similarly, when the source is further away from the preferential pathway, more

332 vapour travels through the soil resulting in more vapour attenuation before reaching the  
333 preferential pathway. As a result of this, comparatively less vapour concentration enters the  
334 preferential pathway and the increase in indoor air vapour concentration abates when compared  
335 to the scenario where the source is close to the preferential pathway. In Figure 6 it can be  
336 observed that when the source was at a depth of 0.5 m from the preferential pathway, a 200%  
337 increase in indoor air concentration was obtained when compared to the same scenario without  
338 preferential pathway which then gradually fell to almost 150% when the depth was increased  
339 to 8 m.



340  
341 Fig. 6. Increase in indoor air concentration with preferential pathway for different depths of  
342 source to preferential pathways.

343 The reduction in indoor air concentration can be attributed to the higher vapour attenuation  
344 occurring in the soil before reaching the preferential pathway due to an increase in depth. As  
345 the depth increases, the vapour concentration entering the preferential pathway decreases and  
346 vice versa. Figure 7 demonstrates the concentration profile of the vadose zone for different  
347 depths of source from the preferential pathway.



348

349 Figure 7. Vapour concentration profiles of the vadose zone for different depths of source from  
 350 preferential pathway

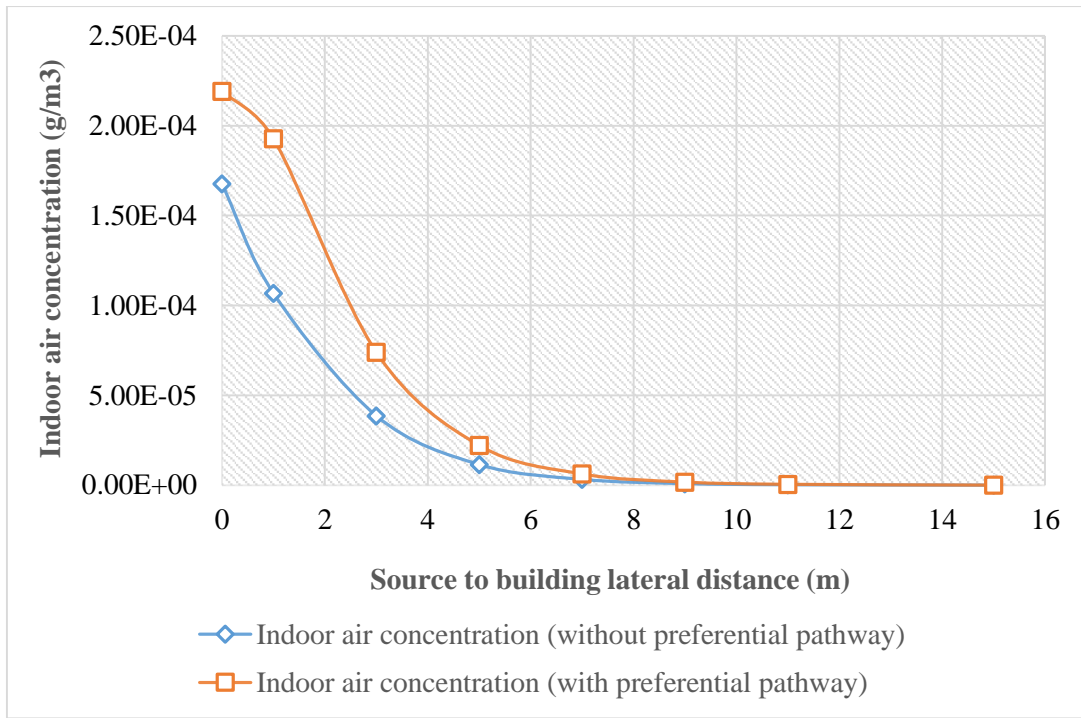
351 **3.2.3. Effect of lateral distance of building from the source**

352 In order to understand the effect of lateral distance in vapour attenuation when preferential  
 353 pathway was present, simulations were conducted to compare the indoor air concentrations with



354 and without preferential pathway. Taken into account here was the building of concern at varied  
355 lateral distances from the edge of the contaminant plume. The simulations were executed  
356 considering the scenario similar to that of the first simulation but with different source to  
357 building lateral distances. A vadose zone of sandy clay soil had a depth of 2.5 m with a highly  
358 permeable preferential pathway of thickness 0.5 m at a depth of 1 m from the ground surface  
359 and the contaminant source of concentration  $1 \text{ g/m}^3$  at a depth further 1 m from the bottom of  
360 the preferential pathway layer. For the scenario without preferential pathway, the vadose zone  
361 is considered homogeneous with sandy clay soil at a depth of 2.5 m from the ground surface.  
362 The input parameters for the simulations are same as those reported in Table 3.

363 It was observed that the indoor air concentration was larger in the presence of the preferential  
364 pathway as expected, but the latter's effect was significant only for a few meters laterally as  
365 shown in Figure 8. As the source to building distance increases, the effect of preferential  
366 pathway in exacerbation of VI reduces until it plays no consequential role in increasing the  
367 indoor air concentration at large lateral distances. This can be attributed to the general tendency  
368 of the vapour to move rapidly in a vertical direction, and thereby crossing the preferential  
369 pathway with least resistance vertically than laterally.



370

371 Figure 8. Indoor air concentration with and without preferential pathway vs source to building  
 372 lateral distances.

373 **3.3. Sensitivity Analysis**

374 The influence of different types of soil texture on the indoor air concentration is investigated  
 375 with the characteristics of 12 typical soils summarised in US EPA database (2012). The total  
 376 porosity, water-filled porosity and intrinsic permeability used for the simulations for 12 typical  
 377 soils are listed in Table 3. Simulations for sensitivity analysis were conducted using a CSM  
 378 where a 0.5 m granular backfill comprising of well graded gravel acting as the preferential  
 379 pathway is at a depth of 1 m below ground surface (bgs) and a TCE contaminant source  $1\text{g/m}^3$   
 380 at a depth of 1 m from the preferential pathway.

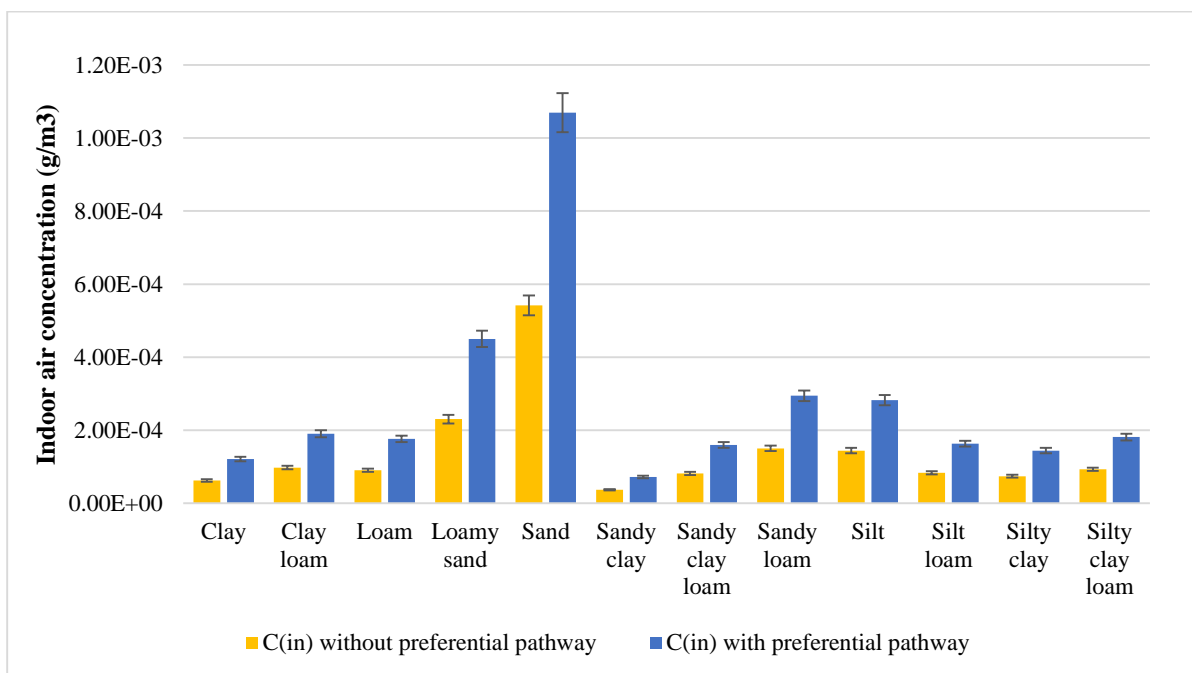
381 Table 3. Soil characteristics for 12 typical soils summarised in US EPA database

<i>Soil Type</i>	<i>Total Porosity</i>	<i>Water-filled porosity</i>	<i>Soil permeability (m<sup>2</sup>)</i>
<i>Clay</i>	0.459	0.215	$2.32 \times 10^{-13}$
<i>Clay Loam</i>	0.442	0.168	$1.29 \times 10^{-13}$
<i>Loam</i>	0.399	0.148	$1.90 \times 10^{-13}$
<i>Loamy sand</i>	0.390	0.076	$1.67 \times 10^{-12}$

<i>Sand</i>	0.375	0.054	$1.02 \times 10^{-11}$
<i>Sandy clay</i>	0.385	0.197	$1.79 \times 10^{-13}$
<i>Sandy clay loam</i>	0.384	0.146	$2.09 \times 10^{-13}$
<i>Sandy loam</i>	0.387	0.103	$6.09 \times 10^{-13}$
<i>Silt</i>	0.489	0.167	$6.92 \times 10^{-13}$
<i>Silt loam</i>	0.439	0.180	$2.89 \times 10^{-13}$
<i>Silty clay</i>	0.481	0.216	$1.52 \times 10^{-13}$
<i>Silty clay loam</i>	0.482	0.198	$1.75 \times 10^{-13}$

382

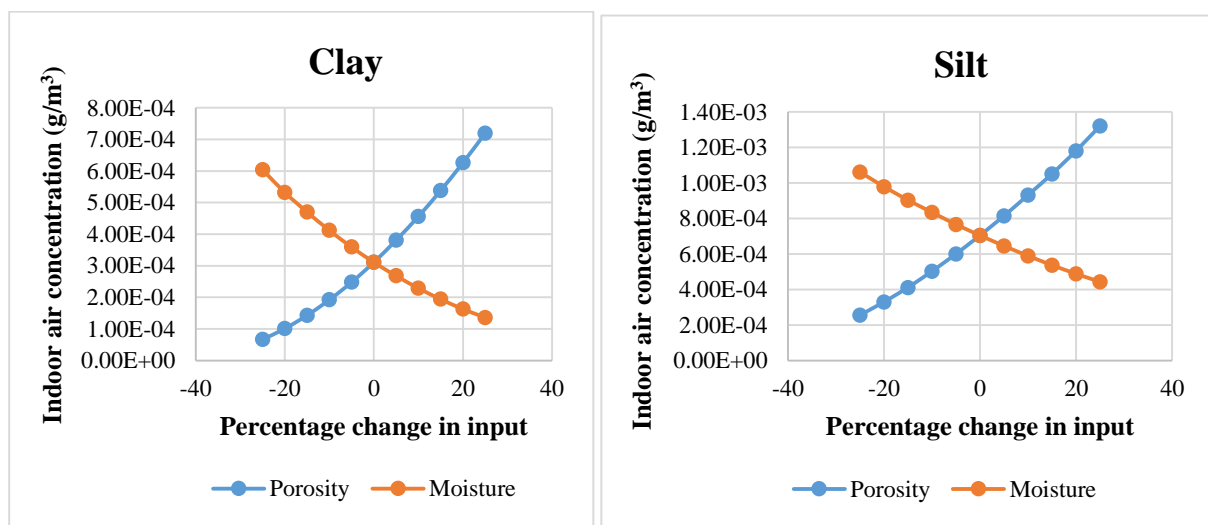
383 Figure 9 shows the indoor air contaminant concentration corresponding to the various types of  
384 soil with different intrinsic permeability in the vadose zone with and without the preferential  
385 pathway. Soils with poor permeability like clay and sandy clay lead to lower indoor air  
386 contaminant concentration as opposed to sand which causes an increased indoor air  
387 contaminant concentration due to its high permeability. An increase of more than one order of  
388 magnitude in indoor air vapour concentration was observed with highly permeable soils in the  
389 vadose zone as compared to soils with low permeability. The presence of highly permeable  
390 preferential pathway of 0.5 m causes almost a two-fold increase in indoor air concentration for  
391 all soil types.



392

393 Figure 9. Simulated indoor air concentrations for 12 typical soils summarised in US EPA  
394 database.

395 To understand the effect of soil porosity and moisture, a one-at-a-time (OAT) sensitivity  
396 analysis technique was conducted in three different types of soils (clay, silt and sand). The  
397 outputs were obtained and compared by varying the input parameters by  $\pm 25\%$  (Ma et al., 2016)  
398 from the default values of clay, silt and sand (given in table 3). Figures 10 (a) (b) and (c) shows  
399 the sensitivity behaviour of soil moisture and soil porosity in this model for clay, silt and sand,  
400 respectively. The sensitivity behaviour of soil moisture and soil porosity is observed to depend  
401 on the soil type. The change in indoor air concentration is almost exponential in clay when  
402 compared to a linear change in sand. So it can be stated here that changes in soil porosity and  
403 moisture content are more sensitive in soils with low permeability. Increase in soil porosity  
404 provides greater passageways for vapour migration, resulting in increased diffusive flux in the  
405 sub-surface and subsequently higher indoor air vapour concentration. Concurrently, an increase  
406 in soil moisture acts as a large resistance to diffusion. As the moisture content in the soil  
407 increases, the effective air diffusivity wanes, resulting in additional partitioning into liquid  
408 phase. Hence the soil gas concentration is reduced which ultimately lowers the indoor air  
409 vapour concentration.

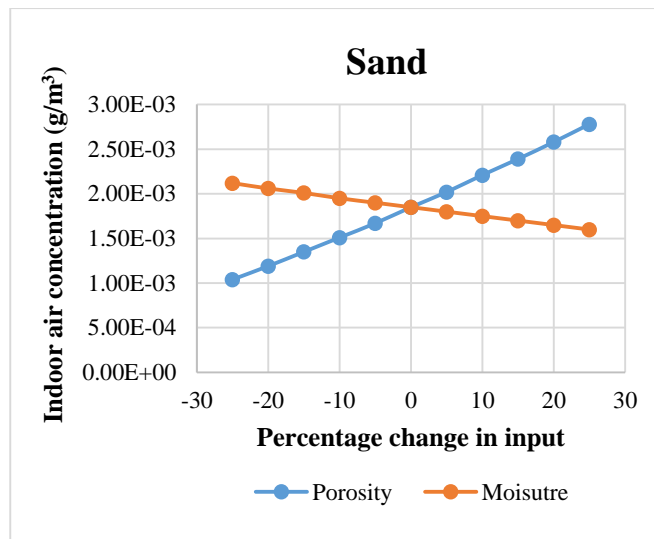


410

411

(a)

(b)



412

413

(c)

414

Figure 10. Changes in indoor air vapour concentration with variations in soil porosity and

415

moisture in (a) clay, (b) silt and (c) sand.

416

### 3.4. Effect of depth of preferential pathway

417

The presence of any kind of high permeability region in the vadose zone – either natural or

418

anthropogenic – can facilitate higher contaminant flux both vertically and laterally owing

419

to its high permeability than the surrounding soils. Figure 11 shows a significant increase

420

in indoor air contaminant concentration for different depths of highly permeable layer in

421

the vadose zone acting as the preferential pathway. From the simulations, a 1 m deep

422

preferential pathway can lead to an almost 70% increase in indoor air contaminant

423

concentration compared to a no preferential pathway scenario. As the depth of preferential

424

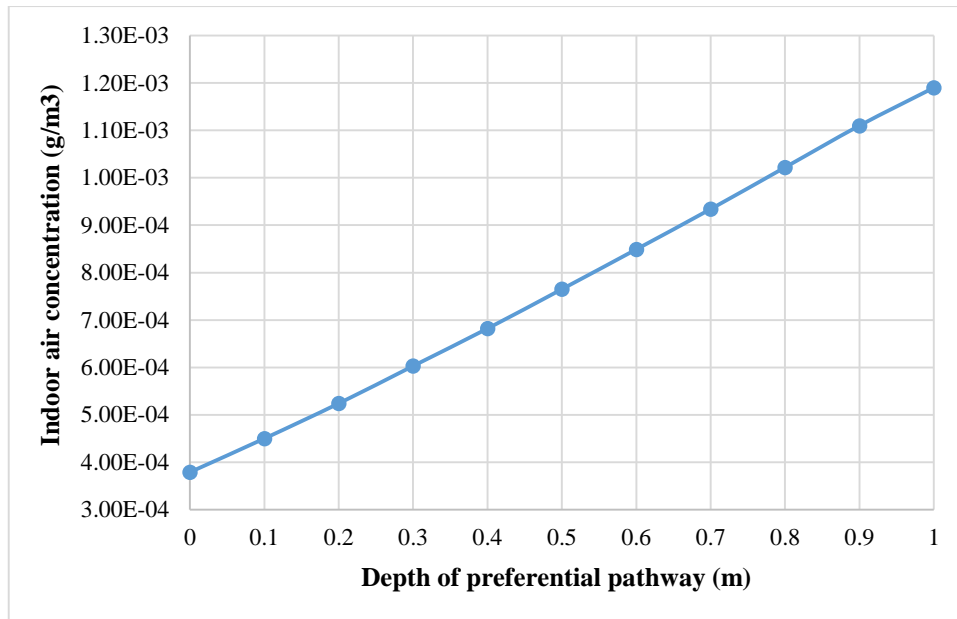
pathway increases, the contaminant vapour has more room for migration with least

425

resistance in the vadose zone resulting in lower attenuation and hence higher indoor air

426

vapour concentration.



427

428

Figure 11. Simulated indoor air contaminant concentration for varying depths of preferential pathway.

429

430

#### 4. Conclusion

431

Detecting the impacts of VI outside the contaminant plume footprint has led to research seeking to understand the role of preferential pathways in VI. Though the majority of studies involving preferential pathways focused on sewer VI investigations, the roles of highly permeable soil layers and backfill materials have rarely been examined. This model was developed to illustrate the role of highly permeable granular soil layers like gravel or crushed rocks used as beddings and backfills for utility lines in exacerbating the indoor air vapour concentrations.

437

Despite some guidance documents suggesting highly permeable soil zones may act as preferential pathways, it is not documented anywhere with sufficient importance suggesting that these pathways might well be addressed by standard VI investigation measures. However from this study, these preferential pathways were found to exacerbate the indoor air concentration depending on the depth of the contaminant plume from the preferential pathway layer. The close proximity of the source to the preferential pathway resulted in an increase of indoor air concentration as high as 200% compared to a no-preferential pathway scenario which

443

444 then decreased to about 150% as the depth of source to preferential pathway increased with  
445 respect to the simulations' parameters. Although it can be considered not a significant increase  
446 in evaluating VI risks, such an increase in indoor air concentration can influence the screening  
447 criteria and response levels of the affected sites by considering it safe or whether an  
448 investigation or intervention is necessary. In the lateral direction, despite the presence of  
449 preferential pathway causing an increased risk of VI, the impact in indoor air concentration is  
450 evident only until a few meters from the plume's edge. As the source to building distance  
451 increases, the preferential pathway seems to play no substantial role in increasing indoor air  
452 concentration at very large lateral distances.

453 Natural soil varies widely in permeability which greatly influences the rate of vapour entry into  
454 buildings. Soils with high permeability like sand result in higher indoor air concentration, of a  
455 greater than one order of magnitude, than soils with low permeability like clay. The presence  
456 of a highly permeable preferential pathway aggravated (in fact doubled) the vapour transport  
457 increasing the indoor air vapour concentration. Vapour transport in the vadose zone is largely  
458 influenced by soil porosity and soil moisture as they influence the effective diffusivity of the  
459 vapour in soil. The sensitivity of these soil parameters is more pronounced in soils with low  
460 permeability.

461 Since the proposed model is based on a CSM scenario of CVI where the building is located  
462 laterally at a distance from the edge of an infinite and uniform contaminant plume, a proper  
463 evaluation of the site needs to be conducted for this model to have feasible applications. This  
464 model can be implemented in places where a highly permeable preferential pathway is prevalent  
465 in the vadose zone which exacerbates VI in the building. As far as limitations are concerned,  
466 this model cannot be used for sites with PVI since biodegradation is not considered here. The  
467 subsurface heterogeneity and the effect of rainfall, snow and changes in groundwater levels  
468 were ignored during the model's development. Hence a proper evaluation is necessary to  
469 understand whether these assumptions are reasonable for sites under consideration.

470 **Declaration of Competing Interests**

471 We declare that we have no financial and personal relationships with other people or  
472 organisations of any kind that could be influencing our work presented in the manuscript titled,  
473 “Two-dimensional vapour intrusion model involving advective transport of vapours with a  
474 highly permeable granular layer in the vadose zone serving as the preferential pathway”.

475 **References**

- 476 2005. Standard Technical Specification for Construction of Sewer Rising Mains. *In:*  
477 CORPORATION, H. W. (ed.).
- 478 ABREU, L. D. & JOHNSON, P. C. 2005. Effect of vapor source– building separation and  
479 building construction on soil vapor intrusion as studied with a three-dimensional  
480 numerical model. *Environmental science & technology*, 39, 4550-4561.
- 481 BECKLEY, L. & MCHUGH, T. 2021. Temporal variability in volatile organic compound  
482 concentrations in sanitary sewers at remediation sites. *Science of The Total  
483 Environment*, 784, 146928.
- 484 CHOI, J.-W., TILLMAN, F. D. & SMITH, J. A. 2002. Relative importance of gas-phase  
485 diffusive and advective trichloroethene (TCE) fluxes in the unsaturated zone under  
486 natural conditions. *Environmental Science & Technology*, 36, 3157-3164.
- 487 DISTLER, M. & MAZIERSKI, P. Soil vapor migration through subsurface utilities. Air &  
488 Waste Management Association, Vapor Intrusion Specialty Conference, 2010.
- 489 EPA, U. 2012. EPA’s Vapor Intrusion Database: Evaluation and Characterization of  
490 Attenuation Factors for Chlorinated Volatile Organic Compounds and Residential  
491 Buildings *In:* RESPONSE, O. O. S. W. A. E. (ed.). Washington, DC.
- 492 GUO, Y., DAHLEN, P. & JOHNSON, P. 2020. Temporal variability of chlorinated volatile  
493 organic compound vapor concentrations in a residential sewer and land drain system  
494 overlying a dilute groundwater plume. *Science of The Total Environment*, 702, 134756.
- 495 GUO, Y., HOLTON, C., LUO, H., DAHLEN, P., GORDER, K., DETTENMAIER, E. &  
496 JOHNSON, P. C. 2015. Identification of alternative vapor intrusion pathways using  
497 controlled pressure testing, soil gas monitoring, and screening model calculations.  
498 *Environmental science & technology*, 49, 13472-13482.
- 499 HOLTON, C., LUO, H., DAHLEN, P., GORDER, K., DETTENMAIER, E. & JOHNSON, P.  
500 C. 2013. Temporal variability of indoor air concentrations under natural conditions in a  
501 house overlying a dilute chlorinated solvent groundwater plume. *Environmental science  
502 & technology*, 47, 13347-13354.
- 503 ITRC 2014. Guidance Document.
- 504 JACOBS, J., JACOBS, O. & PENNELL, K. 2015. One alternate exposure pathway of VOC  
505 vapors from contaminated subsurface environments into indoor air–legacy sewer  
506 plumbing systems. Feature article in the spring 2015 Groundwater Resources  
507 Association of California (GRAC) Newsletter.



508 JOHNSON, P. C. & ETTINGER, R. A. 1991. Heuristic model for predicting the intrusion rate  
509 of contaminant vapors into buildings. *Environmental Science & Technology*, 25, 1445-  
510 1452.

511 MA, J., YAN, G., LI, H. & GUO, S. 2016. Sensitivity and uncertainty analysis for Abreu &  
512 Johnson numerical vapor intrusion model. *Journal of hazardous materials*, 304, 522-  
513 531.

514 MCHUGH, T., BECKLEY, L., SULLIVAN, T., LUTES, C., TRUESDALE, R.,  
515 UPPENCAMP, R., COSKY, B., ZIMMERMAN, J. & SCHUMACHER, B. 2017.  
516 Evidence of a sewer vapor transport pathway at the USEPA vapor intrusion research  
517 duplex. *Science of the Total Environment*, 598, 772-779.

518 MILLINGTON, R. & QUIRK, J. 1961. Permeability of porous solids. *Transactions of the*  
519 *Faraday Society*, 57, 1200-1207.

520 PENNELL, K. G., SCAMMELL, M. K., MCCLEAN, M. D., AMES, J., WELDON, B.,  
521 FRIGUGLIETTI, L., SUUBERG, E. M., SHEN, R., INDEGLIA, P. A. & HEIGER-  
522 BERNAYS, W. J. 2013. Sewer gas: an indoor air source of PCE to consider during  
523 vapor intrusion investigations. *Groundwater Monitoring & Remediation*, 33, 119-126.

524 RIIS, C., CHRISTENSEN, A., HANSEN, M., HUSUM, H. & TERKELSEN, M. Vapor  
525 intrusion through sewer systems: Migration pathways of chlorinated solvents from  
526 groundwater to indoor air. Seventh Battelle International Conference on Remediation  
527 of Chlorinated and Recalcitrant Compounds, Monterey, 2010.

528 ROGHANI, M., JACOBS, O. P., MILLER, A., WILLETT, E. J., JACOBS, J. A., VITERI, C.  
529 R., SHIRAZI, E. & PENNELL, K. G. 2018. Occurrence of chlorinated volatile organic  
530 compounds (VOCs) in a sanitary sewer system: Implications for assessing vapor  
531 intrusion alternative pathways. *Science of The Total Environment*, 616, 1149-1162.

532 SCANLON, B. R., NICOT, J. P. & MASSMANN, J. W. 2002. Soil gas movement in  
533 unsaturated systems. *Soil physics companion*, 389, 297-341.

534 USEPA 2002. OSWER Draft Guidance for Evaluating the Vapor Intrusion to Indoor Air  
535 Pathway from Groundwater and Soils (Subsurface Vapor Intrusion Guidance). *In:*  
536 RESPONSE, O. O. S. W. A. E. (ed.). Washington D.C.: US EPA.

537 USEPA 2015a. OSWER technical guide for assessing and mitigating the vapor intrusion  
538 pathway from subsurface vapor sources to indoor air. *In:* RESPONSE, O. O. S. W. A.  
539 E. (ed.). Washington, DC, USA: OSWER Publication.

540 USEPA 2015b. Technical Guide for Addressing Petroleum Vapor Intrusion at Leaking  
541 Underground Storage Tank Sites. Washington, DC, USA: US Environmental Protection  
542 Agency.

543 VROBLESKY, D. A., PETKEWICH, M. D., LOWERY, M. A. & LANDMEYER, J. E. 2011.  
544 Sewers as a source and sink of chlorinated- solvent groundwater contamination, Marine  
545 Corps Recruit Depot, Parris Island, South Carolina. *Groundwater Monitoring &*  
546 *Remediation*, 31, 63-69.

547 YAO, Y., MAO, F., MA, S., YAO, Y., SUUBERG, E. M. & TANG, X. 2017a. Three-  
548 dimensional simulation of land drains as a preferential pathway for vapor intrusion into  
549 buildings. *Journal of environmental quality*, 46, 1424-1433.

550 YAO, Y., PENNELL, K. G. & SUUBERG, E. M. 2012. Estimation of contaminant subslab  
551 concentration in vapor intrusion. *Journal of hazardous materials*, 231, 10-17.

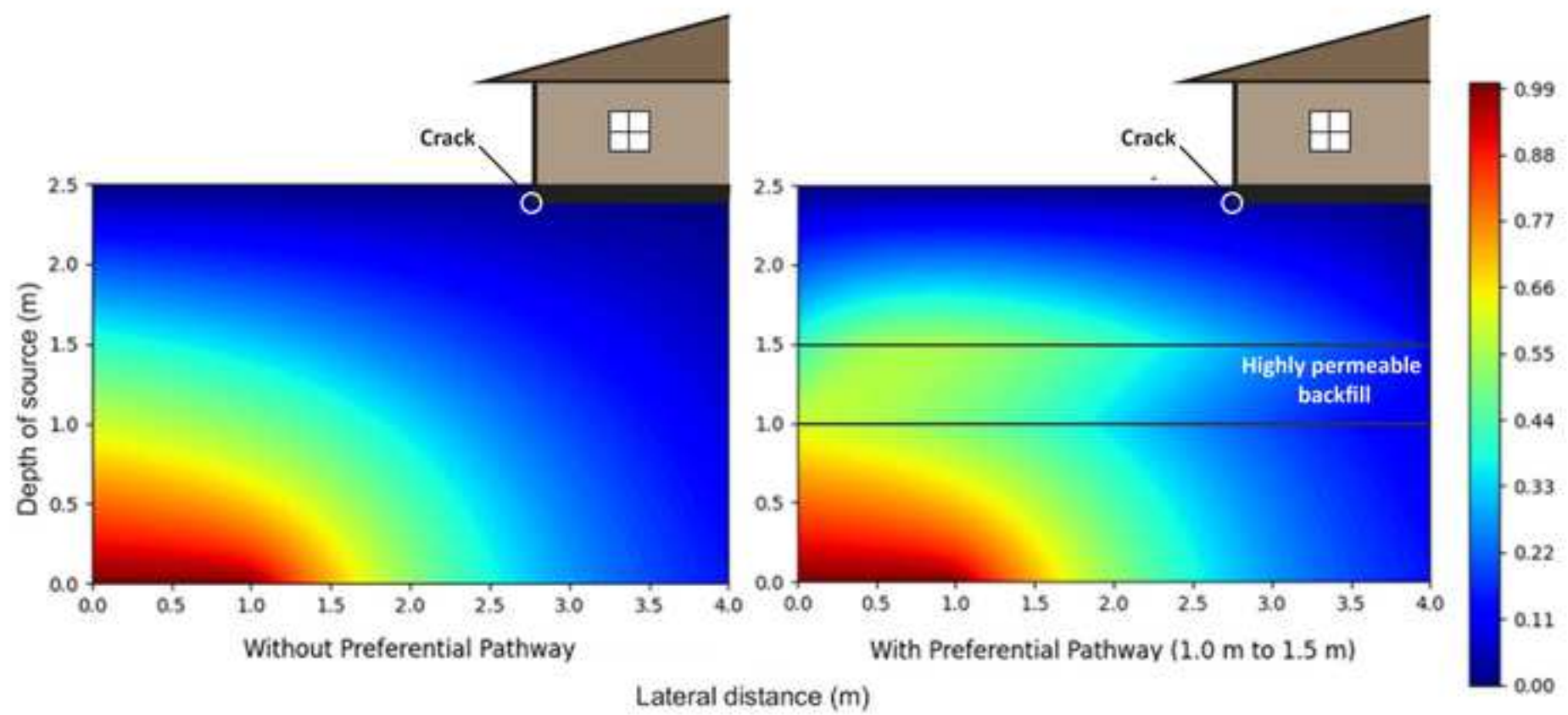
552 YAO, Y., SHEN, R., PENNELL, K. G. & SUUBERG, E. M. 2013. Estimation of contaminant  
553 subslab concentration in vapor intrusion including lateral source–building separation.  
554 *Vadose Zone Journal*, 12.

555 YAO, Y., VERGINELLI, I. & SUUBERG, E. M. 2017b. A two-dimensional analytical model  
556 of vapor intrusion involving vertical heterogeneity. *Water Resour Res*, 53, 4499-4513.

557 YAO, Y., WU, Y., WANG, Y., VERGINELLI, I., ZENG, T., SUUBERG, E. M., JIANG, L.,  
558 WEN, Y. & MA, J. 2015. A petroleum vapor intrusion model involving upward  
559 advective soil gas flow due to methane generation. *Environmental science &*  
560 *technology*, 49, 11577-11585.

561

562



**Two-dimensional vapour intrusion model involving advective transport of vapours with a highly permeable granular layer in the vadose zone serving as the preferential pathway**

**Highlights**

- A 2-D vapour intrusion model to estimate the indoor air concentration is developed
- Effects of highly permeable backfill layers as preferential pathway is considered
- Advection serves the dominant transport mechanism in the preferential pathway layer
- Proximity of the source to preferential pathway affects the indoor air concentration

1     **Two-dimensional chlorinated vapour intrusion model involving advective**  
2     **transport of vapours with a highly permeable granular layer in the vadose**  
3             **zone serving as the preferential pathway**

4     Aravind Unnithan<sup>1</sup>, Dawit Nega Bekele<sup>1,4</sup>, Sreenivasulu Chadalavada<sup>1,3</sup>, Ravi Naidu<sup>1,2</sup>

5

6     <sup>1</sup> Global Centre for Environmental Remediation, The University of Newcastle, University  
7             Drive, Callaghan NSW 2308, Australia

8     <sup>2</sup> CRC CARE, ATC Building, The University of Newcastle, University Drive, Callaghan  
9             NSW 2308, Australia

10    <sup>3</sup> School of Engineering, The University of Southern Queensland, 37 Sinnathamby Boulevard,  
11             University Drive, Springfield Lakes QLD 4300, Australia

12    <sup>4</sup> Douglas Partners Pty Ltd. 439 Montague Road, West End QLD 4101, Australia

13

14

15    Corresponding author:

16    Ravi Naidu <sup>1,2</sup>

17    Email address: [Ravi.Naidu@newcastle.edu.au](mailto:Ravi.Naidu@newcastle.edu.au)

18 **Abstract**

19 Vapour Intrusion (VI) is the process through which volatile organic compounds migrate from  
20 the subsurface source to the soil predominantly by diffusion, entering the overlying buildings  
21 through joints, cracks or other openings. This activity poses potentially serious health hazards  
22 for the occupants. Because of these health risks, recommendations for site closure are often  
23 made by quantifying the VI risks using mathematical models known as ‘Vapour Intrusion  
24 Models’ (VIM). Most of these VIMs seem to overlook the role of preferred pathways like utility  
25 lines, high conductivity zones of soil or rocks, etc., which act as the path of least resistance for  
26 vapour transport thereby increasing vapour intrusion risks. This study presents a two-  
27 dimensional (2-D) chlorinated vapour intrusion (CVI) model which seeks to estimate the  
28 source-to-indoor air concentration attenuation. It takes into account the effects of a highly  
29 permeable utility line embedment as a preferential pathway. The transport of 2-D soil gas is  
30 described using the finite difference method where advection serves as the dominant transport  
31 mechanism in the preferential pathway layer, while diffusion applies to the rest of the vadose  
32 zone. The model returned results comparable with other models for the same input parameters,  
33 and was found to closely replicate the results of 3-D models. The simulations indicate that the  
34 presence of highly permeable utility line embedment and backfill layers do trigger a higher  
35 indoor air concentration compared to a no preferential pathway scenario.

36 **Keywords:** Vapour intrusion; two dimensional model; preferential pathway; chlorinated  
37 hydrocarbons.

38 **Funding**

39 This research did not receive any specific grant from funding agencies in the public,  
40 commercial, or not-for-profit sectors.

41

## 42        **1. Introduction**

43    The conceptual site models (CSMs) help in identifying the pathways for vapour transport in the  
44    vadose zone and its entry into buildings. Conventional CSMs assume a ‘soil VI pathway’ in  
45    which vapours from a subsurface source emanate and diffuse vertically and/or laterally through  
46    the subsurface soil, which then intrudes into the indoor air typically through foundation pores,  
47    cracks or openings (Guo et al., 2015). However, the presence of alternate exposure pathways  
48    in the vadose zone like utility lines, naturally occurring fractures or macro pores, highly  
49    permeable soil layers or backfills etc. had been generally overlooked until recently. These  
50    alternative exposure pathways, known as preferential pathways, intersect with the vapour  
51    source or vapour migration pathways offer least resistance to soil vapour flow, subsequently  
52    and significantly increasing the risk of vapour intrusion (VI) (USEPA, 2002). The majority of  
53    vapour intrusion models (VIMs) currently in use have been developed with conventional CSMs  
54    but have often ignored the potential for vapour entry into indoor air scenarios through utility  
55    corridors, plumbing systems, etc., during VI investigations and developing VIMs. Failure to  
56    incorporate the role of preferential pathways into VI results in inaccurate predictions of indoor  
57    air vapour concentrations and wrong clean-up strategies.

58    The United States Environmental Protection Agency (US EPA) recommended a buffer zone of  
59    about 100 feet (or 30 m) vertically and laterally from the contaminant source, beyond which  
60    buildings can be deemed safe since no significant indoor air concentration had been found in  
61    them at a distance greater than one house lot (USEPA, 2002). Yet, in recent studies, VI impacts  
62    were detected in buildings even outside the footprint of the contaminant plume (Yao et al.,  
63    2017a) due to the presence of preferential pathways which offer little vapour attenuation and  
64    this leads to high indoor air concentrations. Most of the VI through preferential pathways are  
65    related to the interception of compromised or deteriorated sewer systems, primarily designed  
66    to carry wastewater to treatment plants, with the contaminant plume in vadose zone ultimately  
67    resulting in unhindered transport of volatile organic compounds (VOCs) into the indoor air



68 through connected plumbing systems (Jacobs et al., 2015). Several field studies have been  
69 conducted in recent times confirming the role of sewers acting as a preferential pathway for soil  
70 vapour transport, resulting in significant indoor air contaminant concentrations even in  
71 buildings outside the groundwater plume area (Distler and Mazierski, 2010, Riis et al., 2010,  
72 Vroblesky et al., 2011, Pennell et al., 2013, Guo et al., 2015, McHugh et al., 2017, Guo et al.,  
73 2020, Beckley and McHugh, 2021). Additionally, VI episodes without a vadose zone source  
74 can occur from VOCs volatilising from industrial discharges which are directly discharged into  
75 sewer systems which contribute to higher indoor air contaminant concentrations (Roghani et  
76 al., 2018).

77 Many studies conducted on preferential pathways in VI focus on contaminant transport through  
78 sewers, utility tunnels and their associated plumbing conduits. However, the role of highly  
79 permeable soil layers and backfill materials in VI have rarely been investigated. The presence  
80 of any high permeability region in the vadose zone - either natural or anthropogenic - can  
81 function as a preferential pathway in contaminant vapour transport. These regions of high  
82 permeability can occur naturally as gravel layers or fractured rocks which facilitate higher  
83 contaminant flux owing to their higher porosity (USEPA, 2015b). As well, granular fill  
84 materials laid as bedding and embedment to utility lines can cause high contaminant flux  
85 laterally and vertically to the ground surface, and thereby serve as preferential pathways (ITRC,  
86 2014).

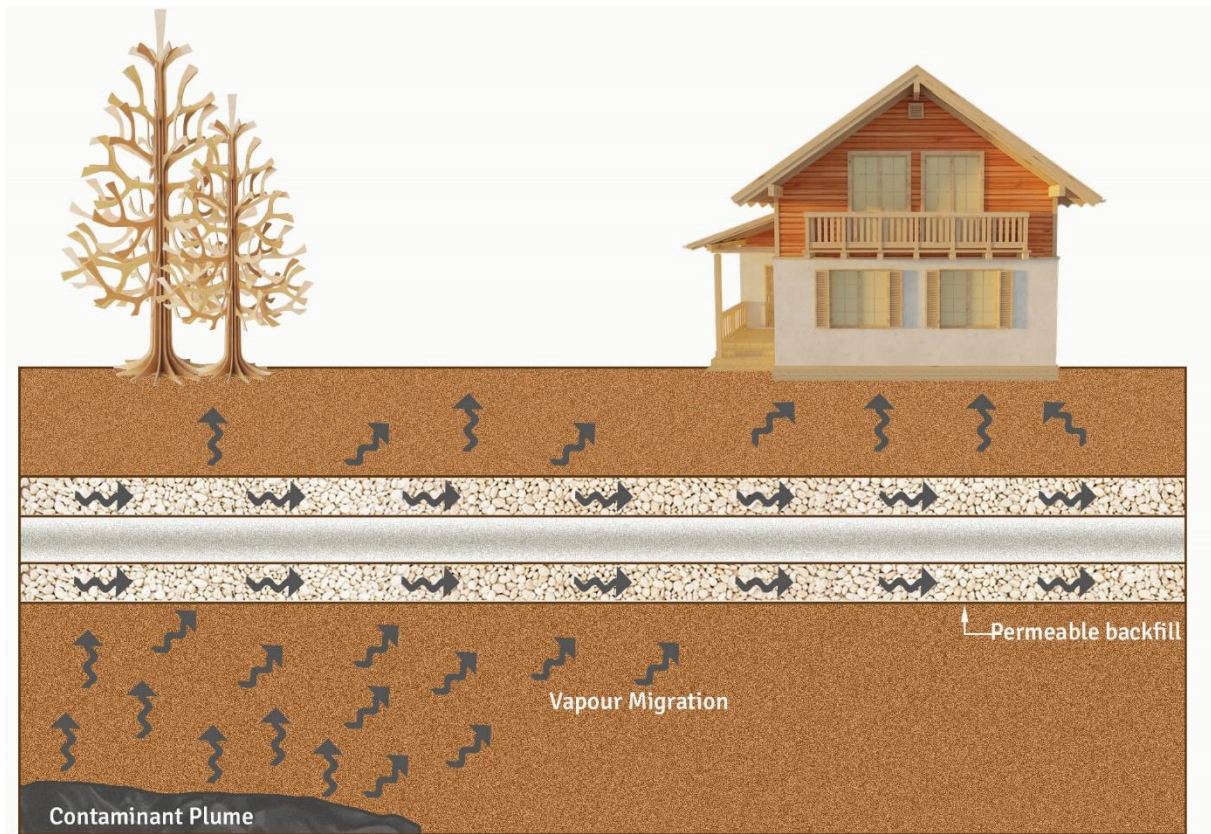
87 The aim of this study is to develop and evaluate a 2-D model in order to estimate the indoor air  
88 concentration at sites contaminated with chlorinated hydrocarbons (CHCs) with a highly  
89 permeable gravel layer acting as a preferential pathway. The numerical model depicts: i) two-  
90 dimensional vapour flux (lateral and vertical directions) of chlorinated hydrocarbon  
91 contaminants; ii) the building of concern laterally situated at a distance from the edge of the  
92 contaminant plume; and iii) the presence of a highly permeable coarse grained soil layer such  
93 as gravel used as bedding for utility lines which act as preferential pathway for vapour transport.

94 This model: firstly, solves partial differential equations of diffusion and advection in the vadose  
95 zone with preferential pathway to estimate the total vapour flux; secondly, has a modular  
96 subroutine for simulating the effect of preferential pathway in vapour transport; and thirdly,  
97 estimates the indoor air concentration by ‘continuous stirred tank reactor method’ as employed  
98 in Johnson and Ettinger’s (hereafter J&E) model. Evaluating the model’s performance was  
99 carried out by comparing it with 1-D, 2-D and 3-D models using hypothetical as well as field  
100 data obtained from particular studies (Holton et al., 2013, Guo et al., 2015, Yao et al., 2017b).

## 101 **2. Methodology**

### 102 **2.1. Model development**

103 The numerical model took two stages to develop. First, a conceptual model was devised  
104 considering: i) the system as two-dimensional; ii) the building of concern placed laterally at a  
105 distance from the edge of the CHC contaminant plume; iii) a coarse grained utility line bedding,  
106 such as gravel, sand or crushed stone with high permeability acting as the path of least resistance  
107 for the contaminant vapour flux; and iv) foundation of the building as slab-on-grade and  
108 simulating the interaction between the sub-surface and the building. The purpose of this  
109 conceptual model is to illustrate the role of highly permeable bedding layers of utility lines in  
110 exacerbating the risk of VI in buildings located laterally at a distance from the edge of the  
111 contaminant plume. The general CSM developed for this study is depicted in Figure 1.



112

113

Figure 1. CSM developed for the study

114

In the second stage of model's development, governing equations were formulated and solved

115

using the central difference scheme of the finite difference method and coded in Python

116

programming language for simulating fate and transport of CHCs from source to the building

117

foundations through sub-surface soil. The vapour entry into the building through the

118

foundations and subsequent indoor air contaminant concentration is calculated using the

119

'continuous stirred tank reactor method' employed in the J&E model (Johnson and Ettinger,

120

1991).

121

Although there are several models which consider two-dimensional vapour transport, most of

122

them assume diffusion is the dominant transport mechanism in the vadose zone but do not take

123

into account the presence of a preferential pathway. Some guidance documents suggest the role

124

of natural and induced high permeability zones in the vadose zone as preferential pathways, for

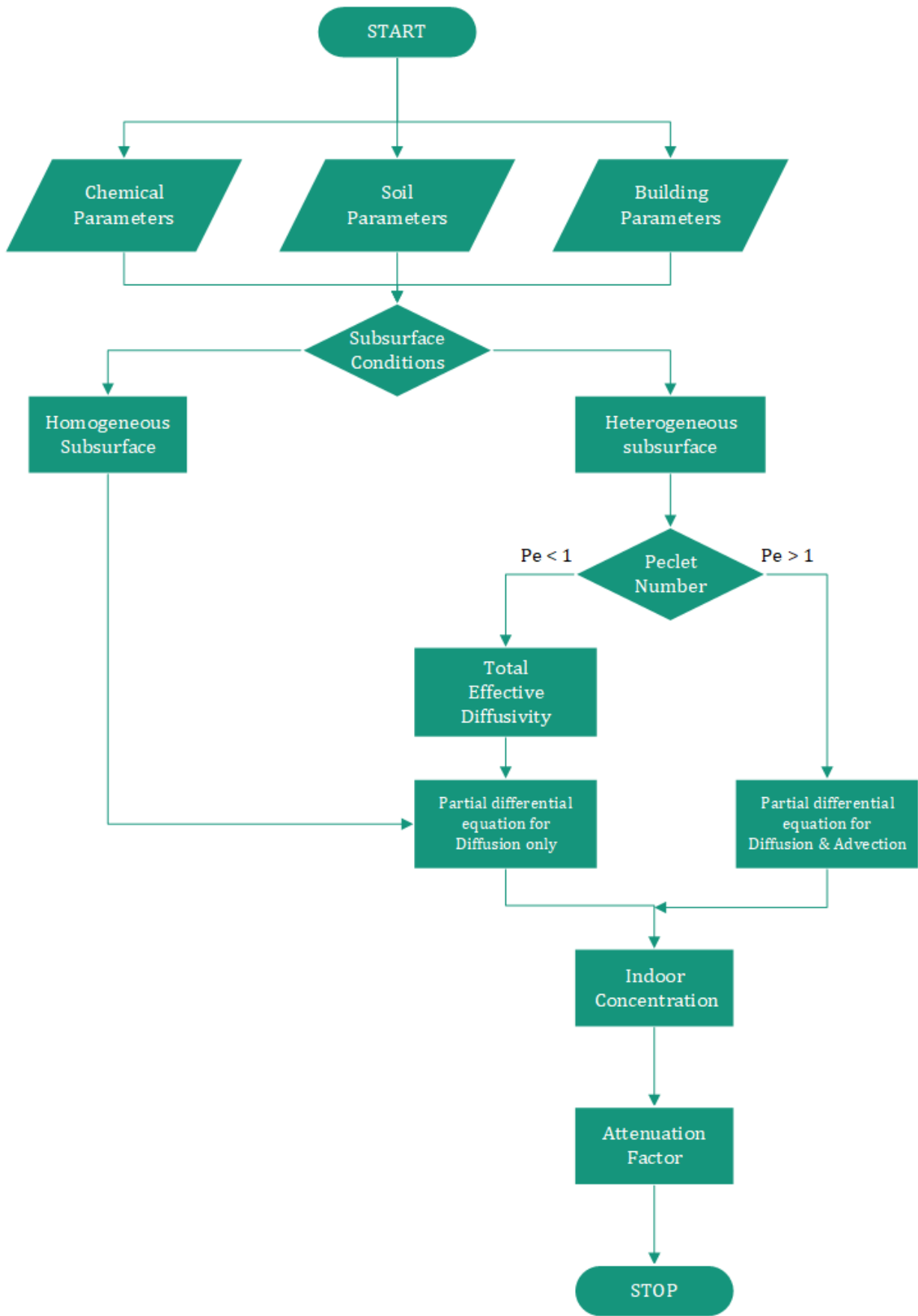
125

instance gravel and sand lenses, vertically fractures rocks, etc., as well as highly permeable

126

bedding or backfill layers of utility lines which are mostly situated close to the surface (USEPA,

127 2015a, ITRC, 2014). However, we know of few studies that have shown vapour migration  
128 through backfills or naturally occurring high permeability zones which this model seeks to  
129 address. When a significant pressure gradient is present, an upward advective soil gas transport  
130 might be induced which can be identified using Peclet number (Pe) (Yao et al., 2015). If  $Pe > 1$ ,  
131 it is assumed that advection will be the dominant transport mechanism but it will be diffusion  
132 if  $Pe < 1$ . The flowchart shown in Figure 2 illustrates the steps involved in developing the 2-D  
133 model for simulation of CHC vapour transport in the presence of a highly permeable  
134 preferential pathway layer. This model calculates the indoor air concentration and attenuation  
135 factor by simulating the vapour transport in the vadose zone. It does this by considering  
136 diffusion as the dominant transport mechanism if  $Pe < 1$  and advection as the dominant transport  
137 mechanism if  $Pe > 1$  in the bedding and backfill layer.



138

139

Figure 2: Overview of the 2-D model process with the preferential pathway

140 The major components involved in the model's methodology are: i) obtaining the vapour flux  
141 and contaminant concentration profile in the vadose zone; ii) determining the dominant  
142 transport mechanism in the backfill and bedding layer by computing  $P_e$ ; iii) calculating vapour  
143 entry into the building using continuous stirred tank reactor method; and iv) computing indoor  
144 air concentration and attenuation factor based on the subsoil and building interaction. The effect  
145 of preferential pathways in three scenarios considered in this study are: i) preferential pathway  
146 closer to the source; ii) preferential pathway equidistant from the source and receptor; and iii)  
147 preferential pathway furthest from the source. Results of these simulations are then compared  
148 with a 'no-preferential pathway' scenario in order to fully understand the role of the highly  
149 permeable bedding layer in exacerbating the VI risk.

150 For refining the numerical model, the following assumptions are made. Firstly, the model  
151 operates under steady state conditions. The source concentration is considered to be constant  
152 and the vapour migration is deemed to be a steady-state process. Although the actual vapour  
153 migration is a transient process, the steady state scenario can express the most hazardous  
154 scenario. Secondly, the subsurface is assumed to be stratified due to the presence of the  
155 preferential pathway and each soil layer is homogeneous. Thirdly, the contaminant  
156 concentration decreases exponentially with lateral distance from the source. Fourthly, the utility  
157 line is leak-proof and does not act as preferential pathway. Fifthly, the effect of biodegradation  
158 is not taken into account since the rate of degradation of TCE is negligible without a growth  
159 substrate like methane (Choi et al., 2002). The vapour concentrations and subsequent indoor air  
160 concentration calculated under these assumptions can be overestimated compared to actual on-  
161 site measurement. Nevertheless, the model can be employed as a screening tool to address the  
162 VI problem with a preferential pathway.

## 163 **2.2. Governing equations and boundary conditions**

### 164 **2.2.1. Transport by diffusion**

165 The vapour transport in the vadose zone is assumed to be steady state diffusion except in the  
 166 highly permeable preferential pathway layer. Since both lateral and vertical movement of the  
 167 contaminant vapours are considered in a two-dimensional soil context, the governing equation  
 168 for the transport of a non-reacting, non-adsorbing vapour through the vadose zone under steady  
 169 state diffusion is explained by Laplace equation as given in eq. (1) (Yao et al., 2017b):

$$170 \left( \frac{\partial^2 C}{\partial x^2} + \frac{\partial^2 C}{\partial y^2} \right) = 0 \quad (1)$$

171 where:  $x$  and  $y$  are lateral and vertical coordinates (m), respectively; and  $C$  denotes the  
 172 contaminant vapour concentration (mg/L).

173 The effective vapour diffusion coefficient of the media,  $D_e$  ( $m^2/s$ ), is calculated using the  
 174 Millington-Quirk equation (1961) as given in eq. (2):

$$175 D_e = D_a \frac{\theta_a^{10/3}}{\theta_T^2} + \frac{D_w \theta_w^{10/3}}{H \theta_T^2} \quad (2)$$

176 where:  $D_a$  is the molecular diffusion coefficient in gas ( $m^2/s$ );  $D_w$  stands for the molecular  
 177 diffusion coefficient in water ( $m^2/s$ );  $\theta_T$ ,  $\theta_a$  &  $\theta_w$  are total porosity, air filled porosity and water  
 178 filled porosity, respectively; and  $H$  is the dimensionless Henry's law constant.

179 In a heterogeneous subsurface with  $n$  layers of soil, a total effective diffusion coefficient can be  
 180 introduced ( $D_{e,tot}$ ) as shown in eq. (3) which transforms the diffusion coefficients of individual  
 181 soil layers of the subsurface into an equivalent homogeneous system (Johnson and Ettinger,  
 182 1991):

$$183 D_{e(tot)} = \frac{L}{\sum_{i=0}^n \frac{d_i}{D_{e(i)}}} \quad (3)$$

184 where:  $L$  is the depth of vadose zone (m);  $d_i$  is the thickness of the  $i$ th layer (m); and  $D_{e(i)}$   
 185 denotes the effective diffusion coefficient of the  $i$ th layer ( $m^2/s$ ).

186

### 187 2.2.2. Transport by advection

188 In preferential subsurface pathways such as utility corridors, highly permeable soils or porous  
189 zones of rocks, the contaminant vapours tend to migrate via advection (USEPA, 2015a). A  
190 relatively small change in partial pressure can trigger significant advective vapour transport  
191 which is larger than the diffusive fluxes (Scanlon et al., 2002). The contaminant vapours reach  
192 the highly permeable granular fill in the vadose zone from the source. Meanwhile the pressure  
193 difference between the subsurface and open ground and the high soil permeability causes a  
194 change in vapour velocity. This can be calculated using eq. (4) as written below:

$$195 \mathbf{u}_g = \frac{K_{bf}}{\mu} \cdot \nabla P_w \quad (4)$$

196 where:  $u_g$  is the average vapour phase velocity (m/s);  $K_{bf}$  is the soil air permeability of the  
197 granular backfill ( $m^2$ );  $\mu$  stands for soil gas viscosity (Pa.s); and  $\nabla P_w$  represents the vapour  
198 pressure gradient in the granular backfill (Pa), which is required as an independent input of the  
199 model.

200 Once the vapour velocity is obtained, the Peclet number can be computed using eq. (5) to  
201 confirm the dominant transport mechanism in the preferential pathway:

$$202 P_e = \frac{u_g \cdot L}{D_{TCE}} \quad (5)$$

203 where:  $u_g$  is the vapour velocity (m/s);  $L$  is the depth of preferential pathway layer (m); and  
204  $D_{TCE}$  is the effective diffusivity of TCE in soil ( $m^2/s$ ).

205 If  $Pe < 1$ , the dominant transport mechanism will be diffusion and the governing equation is  
206 given by eq. (1). If  $Pe > 1$ , the dominant transport mechanism will be advection for which the  
207 governing equation is given by eq. (6) as stated below:

$$208 -\mathbf{u}_g \left( \frac{\partial C}{\partial x} + \frac{\partial C}{\partial y} \right) = \mathbf{0} \quad (6)$$



209 For geological systems with permeability  $> 10^{-9} \text{ m}^2$ , the contaminant transport can be simulated  
210 with advection equation (Yao et al., 2012).

### 211 **2.2.3. Computation of indoor air concentration**

212 The average indoor air concentration is calculated in this model using the ‘continuous stirred  
213 tank reactor’ method as employed in the J&E model. As per the technical VI guidance of US  
214 EPA (2015a), for a building laterally at a distance from the contaminant plume, the soil vapour  
215 concentration obtained from below the foundation closest to the source can help to describe the  
216 worst case scenario underneath the building. Hence the subslab concentration of vapours  
217  $C(x_{ck}, d_s)$  closest to the edge of the contaminant plume is obtained from the simulations and is  
218 employed for the vapour entry and indoor air concentration calculations using eq. (7) to (14).  
219 The sub-slab crack concentration ( $C_{ck}$ ) can be computed using eq. (7) as documented below:

$$220 \quad C_{ck} = \frac{\pi D_e \cdot d_s \cdot t_{ck}}{D_a w_{ck}} C(x_{ck}, d_s) \quad (7)$$

221 where:  $t_{ck}$  is the thickness of the foundation (m);  $w_{ck}$  is the width of the crack (m);  $x_{ck}$  is the  
222 distance of the foundation crack from the edge of contaminant plume and  $d_s$  is the depth of  
223 source from the foundation.

224 The indoor air contaminant concentration ( $C_{in}$ ) can be calculated as a function of sub-slab crack  
225 concentration as given in eq. (8) using a series of empirical equations as stated in eq. (9) to eq.  
226 (14):

$$227 \quad C_{in} = C_{ck} \left( \frac{R_{mix}}{R_{crack} + R_{mix}} \right) \quad (8)$$

228 Where,

$$229 \quad R_{mix} = \frac{1}{L_{mix} \cdot ER} \quad (9)$$

230 and

231  $R_{crack} = \left( R_{mix} - \frac{A_b}{Q_s} \right) (e^{-\varepsilon} - 1)$  (10)

232 with

233  $\varepsilon = \frac{Q_s}{A_b} \frac{t_{ck}}{D_a \eta}$  (11)

234  $\eta = \frac{w_{ck} l_{ck}}{A_b}$  (12)

235  $Q_s = \frac{2\pi K_a \Delta p l_{ck}}{\mu \ln\left(\frac{2d_f}{r_{ck}}\right)}$  (13)

236 and

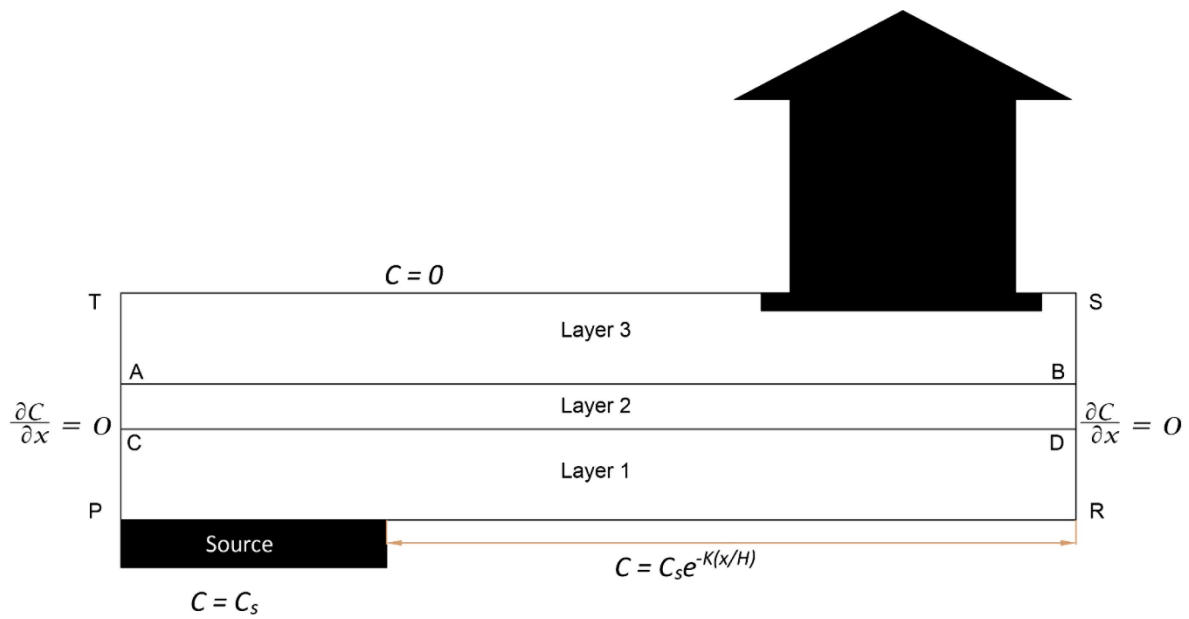
237  $r_{ck} = \frac{\eta A_b}{l_{ck}}$  (14)

238 where:  $L_{mix}$  (m) denotes the height of the building at which contaminant mixing occurs; ER  
 239 (1/hr) is the building air exchange rate;  $A_b$  ( $m^2$ ) stands for the foundation area in contact with  
 240 the soil;  $Q_s$  ( $m^3/s$ ) is the convective soil vapour entry rate into the building;  $d_f$  (m) is the depth  
 241 of foundation below ground surface;  $\eta$  represents the foundation crack fraction;  $l_{ck}$  (m) is the  
 242 foundation perimeter;  $K_a$  ( $m^2$ ) is the soil air permeability;  $\mu$  (Pa.s) is the soil gas viscosity; and  
 243  $\Delta p$  (Pa) is the pressure difference between building and soil.

244 The sub-slab-to-indoor air concentration attenuation factor ( $\alpha$ ), which relates indoor air vapour  
 245 concentration ( $C_{in}$ ) to the source vapour concentration ( $C_s$ ) can be calculated using eq. (15):

246  $\alpha = \frac{C_{in}}{C_s}$  (15)

247 **2.2.4. Boundary conditions**



248

249

Figure 3. Boundary conditions employed for the CSM

250 Figure 3 depicts the boundary conditions for the solution of the transport equations in the vadose

251 zone. The conceptual model assumes concentration at source to be  $C_s$  while the concentration

252 at ground surface is zero. The left-hand and right-hand side boundaries of the domain are

253 assumed to have no flux boundary condition, i.e.  $\frac{\partial C}{\partial x} = 0$  where concentration attenuation is

254 linear. Beyond the edge of the source, the concentration tends towards zero at large lateral

255 distances and the concentration attenuation is exponential which is satisfied by  $C_s e^{-K(\frac{x}{H})}$ ,

256 where:  $x$  is the lateral distance from source (m);  $H$  is the depth of source (m); and  $K$  is the decay

257 rate constant.

258 Boundary condition for advection process in the highly permeable preferential pathway is

259 established by considering the system as three separate layers. The values obtained by solving

260 eq. (1) in layer 1 with the corresponding boundary conditions becomes the boundary condition

261 for layer 2 (CD in fig.3). With  $\nabla P_w$  as independent input in the model, the calculated soil vapour

262 velocity ( $u_g$ ) will determine  $Pe$  which in turn determines the vapour transport mechanism in

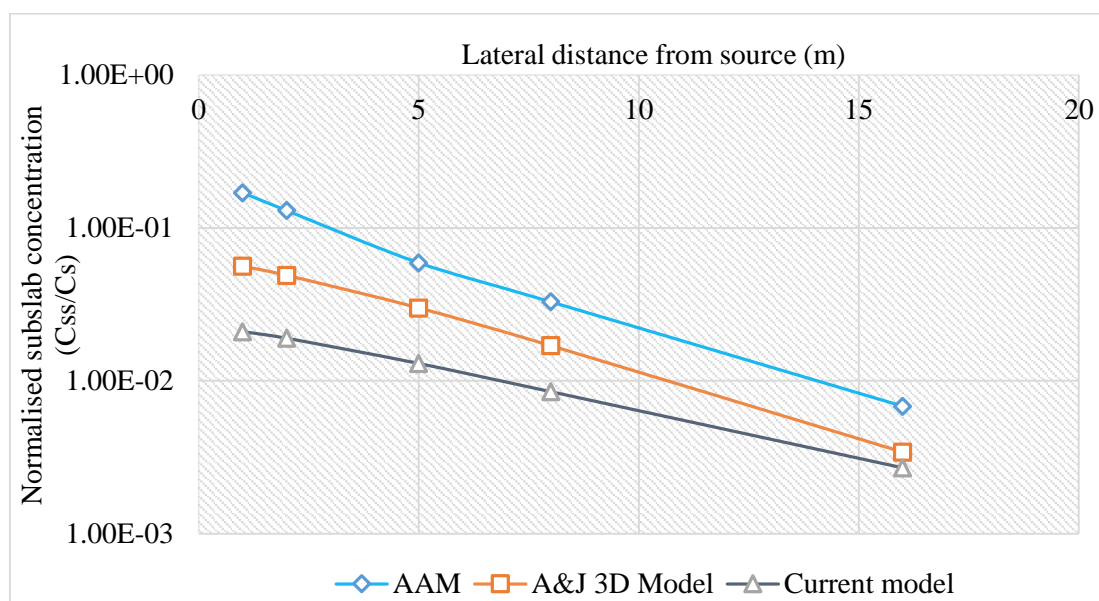
263 layer 2. If  $Pe > 1$ , the transport mechanism will be advection and the system will solve for eq.

264 (6) for the whole layer (until AB in fig. 3). This in turn will serve as the boundary condition for  
265 layer 3 which will solve for diffusion equation for that layer.

### 266 3. Results and Discussion

#### 267 3.1. Comparison with existing models

268 The capability of VI assessment by the developed model is conducted by comparing the results  
269 of the normalised sub-slab concentration obtained from the current model with the results of  
270 analytical approximation method (AAM) (Yao et al., 2013) and Abreu and Johnson's 3-D  
271 model (Abreu and Johnson, 2005). The calculated vapour concentration at the near edge of the  
272 foundation bottom is regarded as the sub-slab concentration. The data adopted for model  
273 comparison is obtained from Yao et al., (2013) for a building foundation depth of 0.2 m and  
274 source depth 8 m for different values of source-building separation. The results of the three  
275 methods are compared in figure 4. With respect to the change in contaminant sub-slab  
276 concentration in lateral direction, the developed model follows the trend of other models,  
277 particularly when compared with the 3-D model, which implies that the developed model may  
278 provide an alternative method of assessing VI risk.



279  
280 Figure 4. The plot of normalised sub-slab concentration ( $C_{ss}/C_s$ ) vs Lateral distance from the  
281 edge of the source for AAM, 3-DM and current model.

282 **3.2.Simulated scenarios**

283 **3.2.1. Effect of preferential pathway**

284 To understand the effect of highly permeable granular fill in the vadose zone in exacerbating  
 285 VI risks, a scenario is simulated by using a granular backfill comprising well graded gravel that  
 286 is 0.5 m in depth. It functions as the preferential pathway at a depth of 1 m from the ground  
 287 surface, where the primary transport mechanism is advection. The building of concern has its  
 288 closest point from the edge of the contaminant plume of concentration 1 g/m<sup>3</sup> at an arbitrarily  
 289 chosen distance of 3 m. The rest of the vadose zone other than the preferential pathway is  
 290 assumed to consist of sandy clay where diffusion is assumed to be the primary transport  
 291 mechanism. The specifications related to pipe embedment and backfilling is consistent with  
 292 Standard drawings SCP-1000 and SCP-1001 of the Standard Technical Specifications for  
 293 Construction of Sewer Rising Mains by Hunter Water Corporation (2005).This is then  
 294 compared to a ‘no-preferential pathway’ scenario where the vadose zone is considered  
 295 homogeneous with sandy clay soil where diffusion is the only soil transport mechanism.  
 296 Biodegradation is not accounted for in the simulations since the contaminant of interest is TCE  
 297 which is normally difficult to biodegrade in soil. The input parameters used in the simulations  
 298 are reported in Table 1.

299 Table 1. Input parameters for the model simulations.

<i>Chemical Parameters</i>		<i>Unit</i>	<i>Value</i>
<i>Source vapour concentration</i>	C <sub>s</sub>	g/m <sup>3</sup>	1
<i>Diffusion coefficient in air</i>	D <sub>a</sub>	m <sup>2</sup> /s	7.90E-06
<i>Diffusion coefficient in water</i>	D <sub>w</sub>	m <sup>2</sup> /s	9.10E-10
<i>Henry’s law constant</i>	H	-	0.403
<i>Soil gas viscosity</i>	μ	Pa.s	5.32E-04
<b><i>Soil Parameters</i></b>			
<i>Total Porosity</i>	Θ <sub>T</sub>	-	0.385
<i>Air filled porosity</i>	Θ <sub>a</sub>	-	0.188
<i>Water filled porosity</i>	Θ <sub>w</sub>	-	0.197
<i>Soil air permeability</i>	K <sub>a</sub>	m <sup>2</sup>	1.70E-13
<b><i>Granular backfill soil parameters</i></b>			

<i>Depth of backfill</i>	ds	m	0.5
<i>Total Porosity</i>	$\Theta_T$	-	0.5
<i>Air filled porosity</i>	$\Theta_a$	-	0.49
<i>Water filled porosity</i>	$\Theta_w$	-	0.01
<i>Soil air permeability</i>	$K_a$	m <sup>2</sup>	1.00E-09
<b><i>Building parameters</i></b>			
<i>Width of foundation slab</i>		m	10
<i>Foundation footprint area</i>	$A_b$	m <sup>2</sup>	100
<i>Depth of foundation below grade</i>	$d_f$	m	0.3
<i>Thickness of foundation crack</i>	$t_{ck}$	m	0.1
<i>Width of foundation crack</i>	$w_{ck}$	m	0.001
<i>Foundation perimeter</i>	$l_{ck}$	m	40
<i>Building height</i>	$L_{mix}$	m	3
<i>Building Air exchange rate</i>	ER	h <sup>-1</sup>	0.5
<i>Soil and building pressure difference</i>	$\Delta p$	Pa	5

300

301 From the simulations, it was observed that there was a considerable increase, virtually double  
302 the amount, in sub-slab as well as indoor air concentrations in the presence of a highly  
303 permeable preferential pathway layer when compared to the ‘no-preferential pathway’ scenario.  
304 Table 2 shows the contrasts in vapour concentration in the sub-slab and indoor air and the  
305 attenuation factor with and without the preferential pathway. Based on these results, it is clearly  
306 evident that the presence of preferential pathway indeed increases the potential risk of VI.

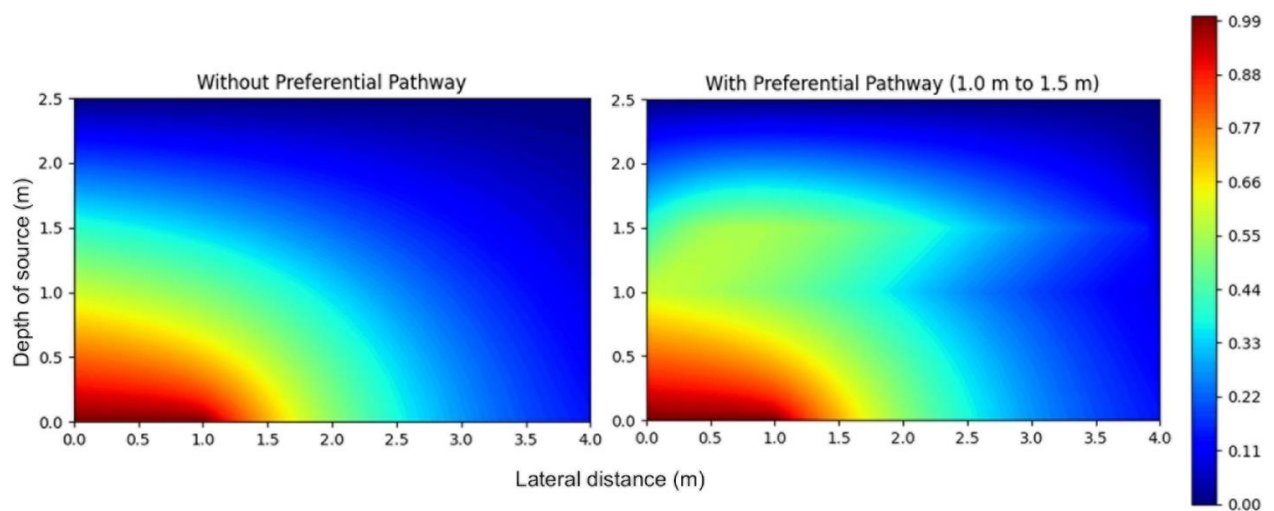
307 Table 2. Comparison of sub-slab concentration, indoor air concentration and attenuation factor  
308 with and without the preferential pathway for different scenarios.

	<i>Without preferential pathway</i>	<i>With preferential pathway</i>
<i>Source concentration (g/m<sup>3</sup>)</i>	1	1
<i>Sub-slab concentration (g/m<sup>3</sup>)</i>	0.025	0.048
<i>Indoor air concentration (g/m<sup>3</sup>)</i>	3.86E-05	7.40E-05
<i>Attenuation factor (<math>\alpha</math>)</i>	3.86E-05	7.40E-05

309

310 This increase in indoor air contaminant concentration can be attributed to the limited attenuation  
311 occurring in the preferential pathway. Advection is assumed to be the dominant transport  
312 mechanism in the preferential pathway layer, so the vapour movement occurs at a faster rate.

313 This is comparable to the rest of the vadose zone where vapour transport occurs due to diffusion,  
314 hence offering the least resistance for soil gas transport and subsequently less attenuation.  
315 Figure 5 presents the vapour concentration profile in the vadose zone which shows the increase  
316 in vapour concentration in the preferential pathway layer as opposed to that of a ‘no-preferential  
317 pathway’ scenario. It proves that the preferential pathway offers the least resistance to vapour  
318 transport in the vadose zone and ultimately results in exacerbation of VI.

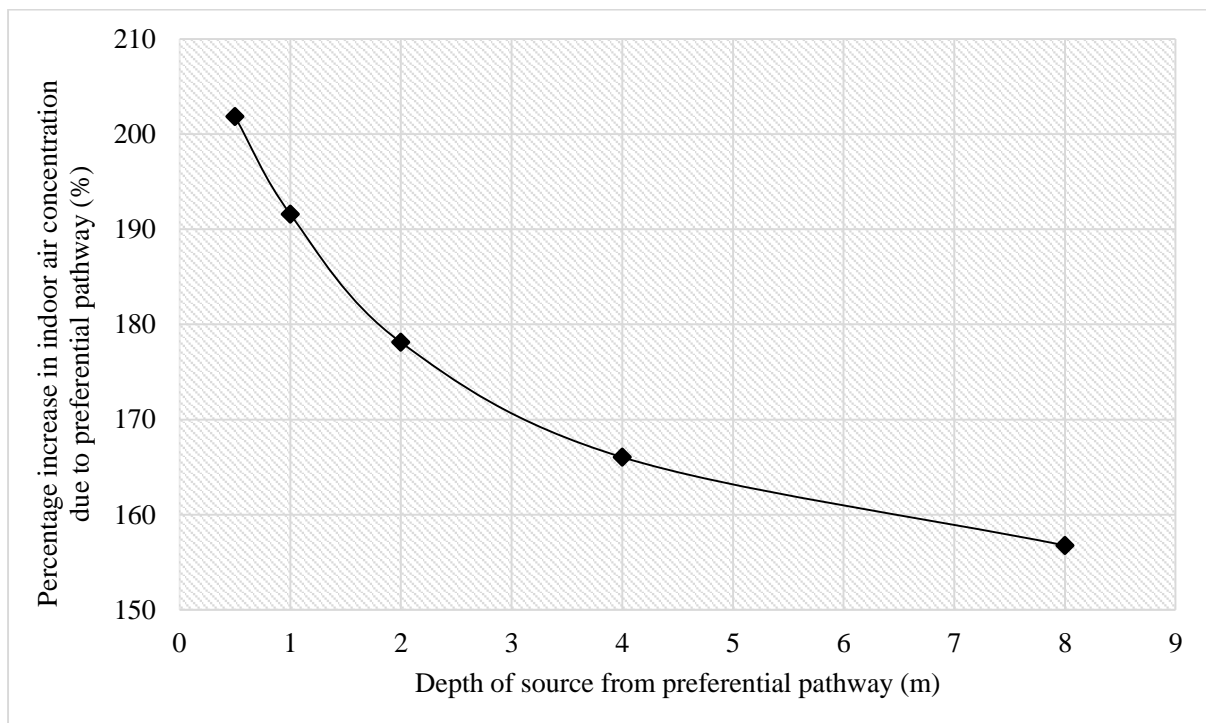


319  
320 Fig. 5: Comparison of vapour concentration profile in the vadose zone with and without the  
321 preferential pathway for the same scenario.

### 322 3.2.2. Influence of depth of source from preferential pathway

323 Simulations were conducted to understand the effect of proximity of the source to the  
324 preferential pathway by varying the depth of source (0.5 m, 1 m, 2 m, 4 m & 8 m) from the  
325 preferential pathway, retaining the remainder of the vadose zone conditions and the input  
326 parameters the same as that of the previous simulation. The closer the source is to the  
327 preferential pathway, the distance of vapour transport in soil before reaching the preferential  
328 pathway diminishes, resulting in less vapour attenuation. This causes a high vapour  
329 concentration to enter the preferential pathway which then travels with comparatively least  
330 resistance till the upper layer of soil with lesser attenuation, leading to an increase in indoor air  
331 concentration. Similarly, when the source is further away from the preferential pathway, more

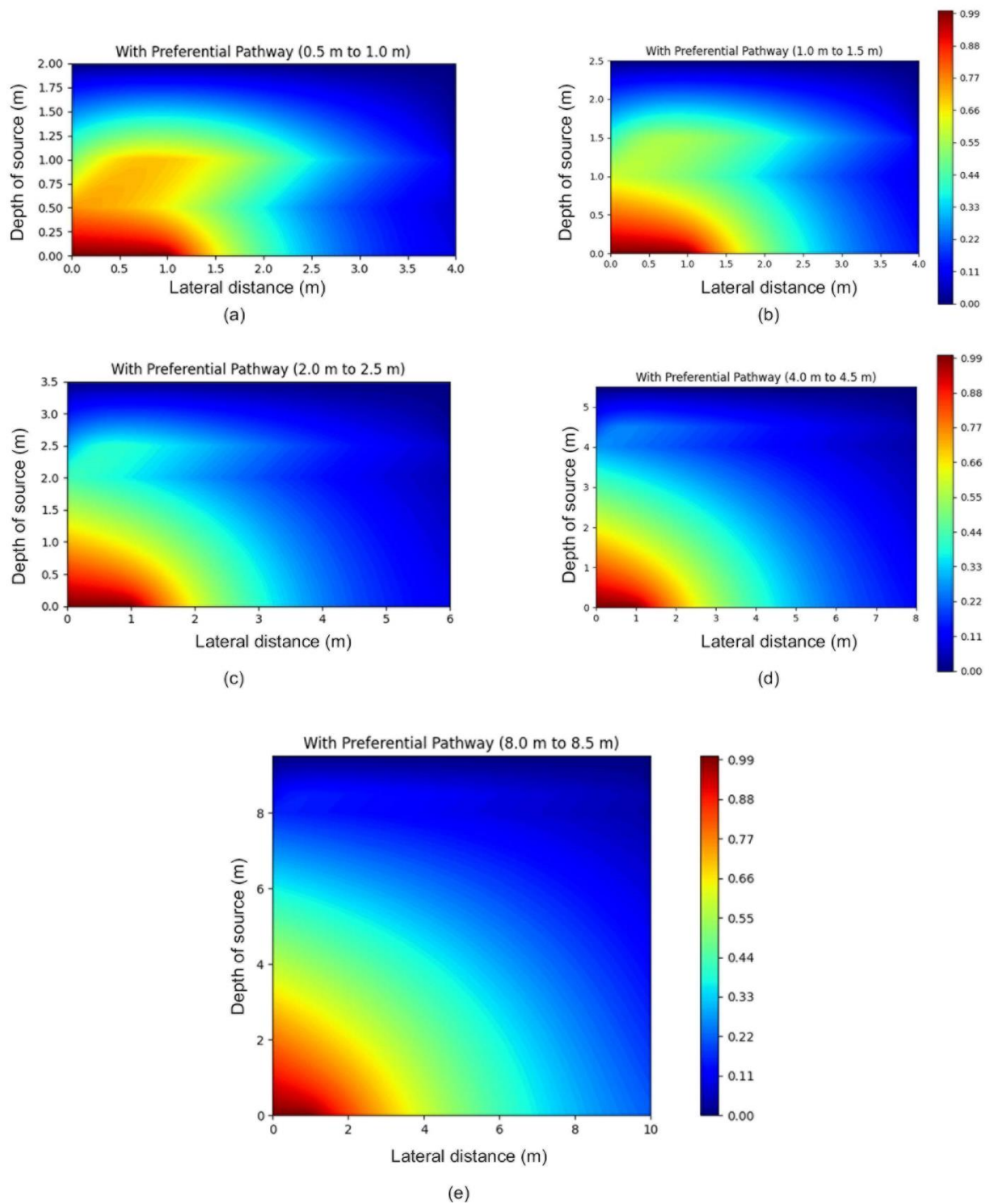
332 vapour travels through the soil resulting in more vapour attenuation before reaching the  
333 preferential pathway. As a result of this, comparatively less vapour concentration enters the  
334 preferential pathway and the increase in indoor air vapour concentration abates when compared  
335 to the scenario where the source is close to the preferential pathway. In Figure 6 it can be  
336 observed that when the source was at a depth of 0.5 m from the preferential pathway, a 200%  
337 increase in indoor air concentration was obtained when compared to the same scenario without  
338 preferential pathway which then gradually fell to almost 150% when the depth was increased  
339 to 8 m.



340  
341 Fig. 6. Increase in indoor air concentration with preferential pathway for different depths of  
342 source to preferential pathways.

343 The reduction in indoor air concentration can be attributed to the higher vapour attenuation  
344 occurring in the soil before reaching the preferential pathway due to an increase in depth. As  
345 the depth increases, the vapour concentration entering the preferential pathway decreases and  
346 vice versa. Figure 7 demonstrates the concentration profile of the vadose zone for different  
347 depths of source from the preferential pathway.





348

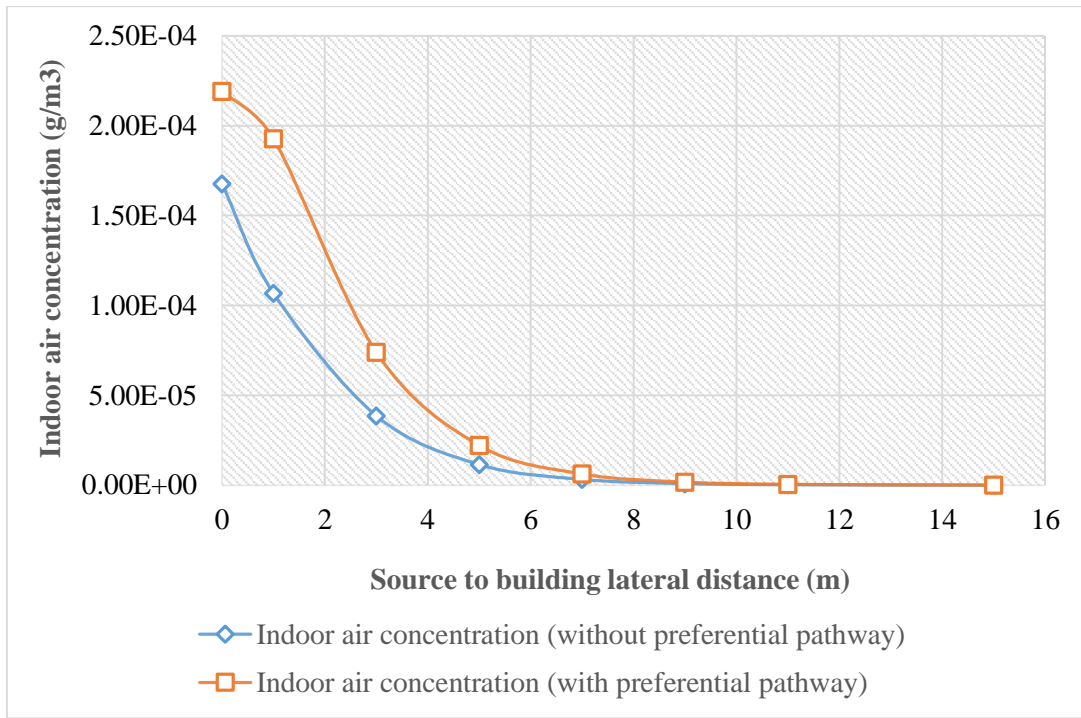
349 Figure 7. Vapour concentration profiles of the vadose zone for different depths of source from  
 350 preferential pathway

351 **3.2.3. Effect of lateral distance of building from the source**

352 In order to understand the effect of lateral distance in vapour attenuation when preferential  
 353 pathway was present, simulations were conducted to compare the indoor air concentrations with

354 and without preferential pathway. Taken into account here was the building of concern at varied  
355 lateral distances from the edge of the contaminant plume. The simulations were executed  
356 considering the scenario similar to that of the first simulation but with different source to  
357 building lateral distances. A vadose zone of sandy clay soil had a depth of 2.5 m with a highly  
358 permeable preferential pathway of thickness 0.5 m at a depth of 1 m from the ground surface  
359 and the contaminant source of concentration  $1 \text{ g/m}^3$  at a depth further 1 m from the bottom of  
360 the preferential pathway layer. For the scenario without preferential pathway, the vadose zone  
361 is considered homogeneous with sandy clay soil at a depth of 2.5 m from the ground surface.  
362 The input parameters for the simulations are same as those reported in Table 3.

363 It was observed that the indoor air concentration was larger in the presence of the preferential  
364 pathway as expected, but the latter's effect was significant only for a few meters laterally as  
365 shown in Figure 8. As the source to building distance increases, the effect of preferential  
366 pathway in exacerbation of VI reduces until it plays no consequential role in increasing the  
367 indoor air concentration at large lateral distances. This can be attributed to the general tendency  
368 of the vapour to move rapidly in a vertical direction, and thereby crossing the preferential  
369 pathway with least resistance vertically than laterally.



370

371 Figure 8. Indoor air concentration with and without preferential pathway vs source to building  
 372 lateral distances.

373 **3.3. Sensitivity Analysis**

374 The influence of different types of soil texture on the indoor air concentration is investigated  
 375 with the characteristics of 12 typical soils summarised in US EPA database (2012). The total  
 376 porosity, water-filled porosity and intrinsic permeability used for the simulations for 12 typical  
 377 soils are listed in Table 3. Simulations for sensitivity analysis were conducted using a CSM  
 378 where a 0.5 m granular backfill comprising of well graded gravel acting as the preferential  
 379 pathway is at a depth of 1 m below ground surface (bgs) and a TCE contaminant source  $1\text{g/m}^3$   
 380 at a depth of 1 m from the preferential pathway.

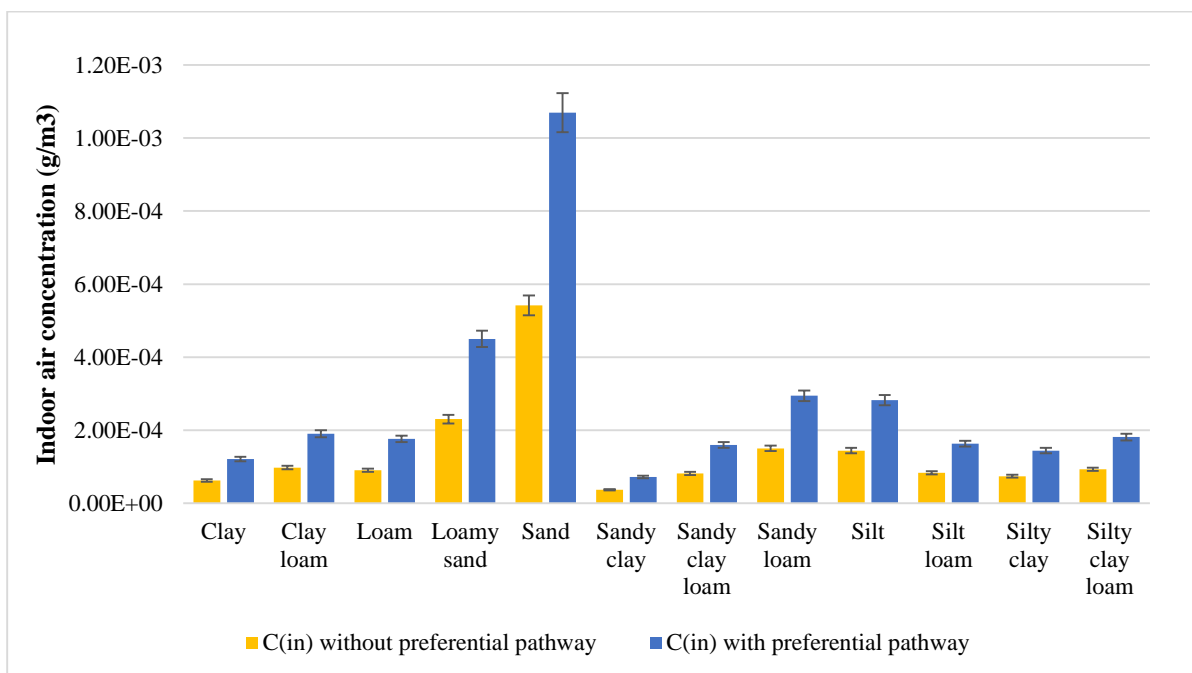
381 Table 3. Soil characteristics for 12 typical soils summarised in US EPA database

<i>Soil Type</i>	<i>Total Porosity</i>	<i>Water-filled porosity</i>	<i>Soil permeability (m<sup>2</sup>)</i>
<i>Clay</i>	0.459	0.215	$2.32 \times 10^{-13}$
<i>Clay Loam</i>	0.442	0.168	$1.29 \times 10^{-13}$
<i>Loam</i>	0.399	0.148	$1.90 \times 10^{-13}$
<i>Loamy sand</i>	0.390	0.076	$1.67 \times 10^{-12}$

<i>Sand</i>	0.375	0.054	$1.02 \times 10^{-11}$
<i>Sandy clay</i>	0.385	0.197	$1.79 \times 10^{-13}$
<i>Sandy clay loam</i>	0.384	0.146	$2.09 \times 10^{-13}$
<i>Sandy loam</i>	0.387	0.103	$6.09 \times 10^{-13}$
<i>Silt</i>	0.489	0.167	$6.92 \times 10^{-13}$
<i>Silt loam</i>	0.439	0.180	$2.89 \times 10^{-13}$
<i>Silty clay</i>	0.481	0.216	$1.52 \times 10^{-13}$
<i>Silty clay loam</i>	0.482	0.198	$1.75 \times 10^{-13}$

382

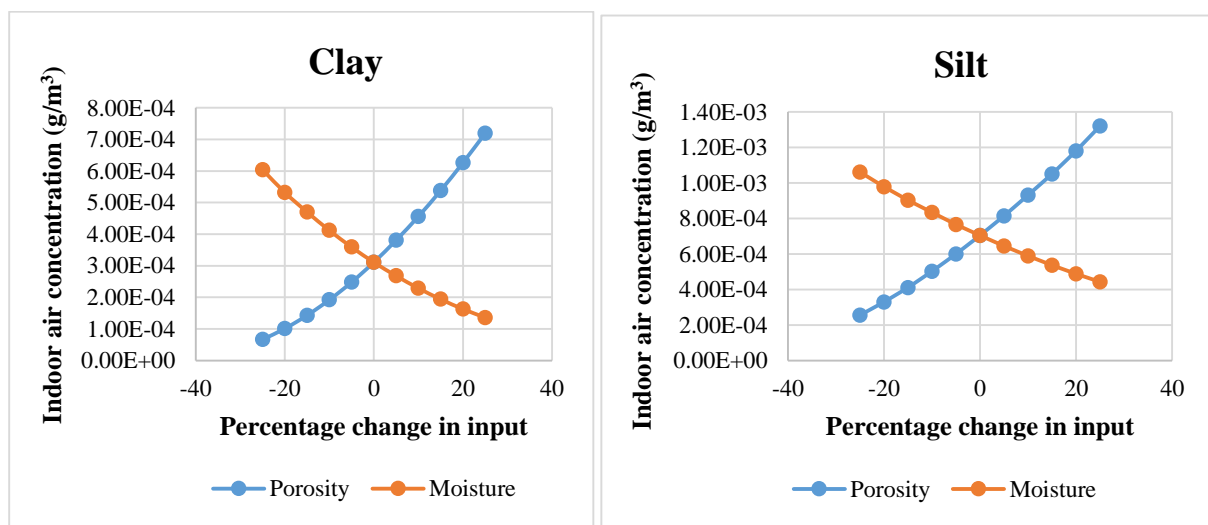
383 Figure 9 shows the indoor air contaminant concentration corresponding to the various types of  
 384 soil with different intrinsic permeability in the vadose zone with and without the preferential  
 385 pathway. Soils with poor permeability like clay and sandy clay lead to lower indoor air  
 386 contaminant concentration as opposed to sand which causes an increased indoor air  
 387 contaminant concentration due to its high permeability. An increase of more than one order of  
 388 magnitude in indoor air vapour concentration was observed with highly permeable soils in the  
 389 vadose zone as compared to soils with low permeability. The presence of highly permeable  
 390 preferential pathway of 0.5 m causes almost a two-fold increase in indoor air concentration for  
 391 all soil types.



392

393 Figure 9. Simulated indoor air concentrations for 12 typical soils summarised in US EPA  
394 database.

395 To understand the effect of soil porosity and moisture, a one-at-a-time (OAT) sensitivity  
396 analysis technique was conducted in three different types of soils (clay, silt and sand). The  
397 outputs were obtained and compared by varying the input parameters by  $\pm 25\%$  (Ma et al., 2016)  
398 from the default values of clay, silt and sand (given in table 3). Figures 10 (a) (b) and (c) shows  
399 the sensitivity behaviour of soil moisture and soil porosity in this model for clay, silt and sand,  
400 respectively. The sensitivity behaviour of soil moisture and soil porosity is observed to depend  
401 on the soil type. The change in indoor air concentration is almost exponential in clay when  
402 compared to a linear change in sand. So it can be stated here that changes in soil porosity and  
403 moisture content are more sensitive in soils with low permeability. Increase in soil porosity  
404 provides greater passageways for vapour migration, resulting in increased diffusive flux in the  
405 sub-surface and subsequently higher indoor air vapour concentration. Concurrently, an increase  
406 in soil moisture acts as a large resistance to diffusion. As the moisture content in the soil  
407 increases, the effective air diffusivity wanes, resulting in additional partitioning into liquid  
408 phase. Hence the soil gas concentration is reduced which ultimately lowers the indoor air  
409 vapour concentration.

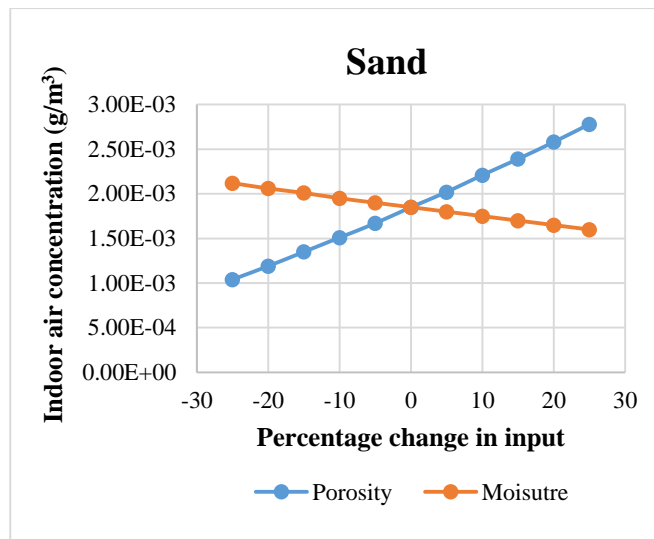


410

411

(a)

(b)



412

413

(c)

414

Figure 10. Changes in indoor air vapour concentration with variations in soil porosity and

415

moisture in (a) clay, (b) silt and (c) sand.

416

### 3.4. Effect of depth of preferential pathway

417

The presence of any kind of high permeability region in the vadose zone – either natural or

418

anthropogenic – can facilitate higher contaminant flux both vertically and laterally owing

419

to its high permeability than the surrounding soils. Figure 11 shows a significant increase

420

in indoor air contaminant concentration for different depths of highly permeable layer in

421

the vadose zone acting as the preferential pathway. From the simulations, a 1 m deep

422

preferential pathway can lead to an almost 70% increase in indoor air contaminant

423

concentration compared to a no preferential pathway scenario. As the depth of preferential

424

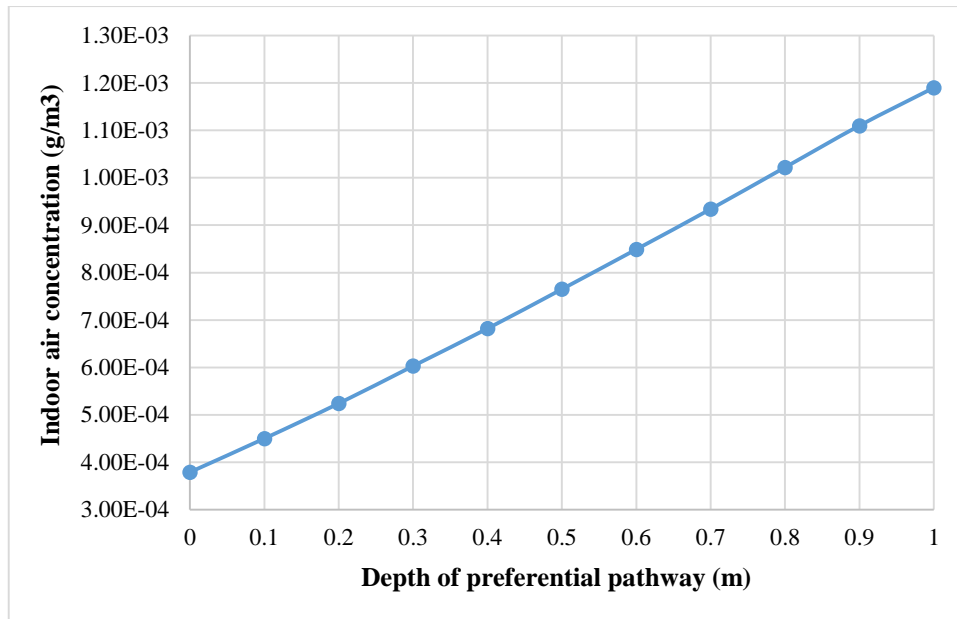
pathway increases, the contaminant vapour has more room for migration with least

425

resistance in the vadose zone resulting in lower attenuation and hence higher indoor air

426

vapour concentration.



427

428

Figure 11. Simulated indoor air contaminant concentration for varying depths of preferential pathway.

429

430

#### 4. Conclusion

431

Detecting the impacts of VI outside the contaminant plume footprint has led to research seeking to understand the role of preferential pathways in VI. Though the majority of studies involving preferential pathways focused on sewer VI investigations, the roles of highly permeable soil layers and backfill materials have rarely been examined. This model was developed to illustrate the role of highly permeable granular soil layers like gravel or crushed rocks used as beddings and backfills for utility lines in exacerbating the indoor air vapour concentrations.

437

Despite some guidance documents suggesting highly permeable soil zones may act as preferential pathways, it is not documented anywhere with sufficient importance suggesting that these pathways might well be addressed by standard VI investigation measures. However from this study, these preferential pathways were found to exacerbate the indoor air concentration depending on the depth of the contaminant plume from the preferential pathway layer. The close proximity of the source to the preferential pathway resulted in an increase of indoor air concentration as high as 200% compared to a no-preferential pathway scenario which

443

444 then decreased to about 150% as the depth of source to preferential pathway increased with  
445 respect to the simulations' parameters. Although it can be considered not a significant increase  
446 in evaluating VI risks, such an increase in indoor air concentration can influence the screening  
447 criteria and response levels of the affected sites by considering it safe or whether an  
448 investigation or intervention is necessary. In the lateral direction, despite the presence of  
449 preferential pathway causing an increased risk of VI, the impact in indoor air concentration is  
450 evident only until a few meters from the plume's edge. As the source to building distance  
451 increases, the preferential pathway seems to play no substantial role in increasing indoor air  
452 concentration at very large lateral distances.

453 Natural soil varies widely in permeability which greatly influences the rate of vapour entry into  
454 buildings. Soils with high permeability like sand result in higher indoor air concentration, of a  
455 greater than one order of magnitude, than soils with low permeability like clay. The presence  
456 of a highly permeable preferential pathway aggravated (in fact doubled) the vapour transport  
457 increasing the indoor air vapour concentration. Vapour transport in the vadose zone is largely  
458 influenced by soil porosity and soil moisture as they influence the effective diffusivity of the  
459 vapour in soil. The sensitivity of these soil parameters is more pronounced in soils with low  
460 permeability.

461 Since the proposed model is based on a CSM scenario of CVI where the building is located  
462 laterally at a distance from the edge of an infinite and uniform contaminant plume, a proper  
463 evaluation of the site needs to be conducted for this model to have feasible applications. This  
464 model can be implemented in places where a highly permeable preferential pathway is prevalent  
465 in the vadose zone which exacerbates VI in the building. As far as limitations are concerned,  
466 this model cannot be used for sites with PVI since biodegradation is not considered here. The  
467 subsurface heterogeneity and the effect of rainfall, snow and changes in groundwater levels  
468 were ignored during the model's development. Hence a proper evaluation is necessary to  
469 understand whether these assumptions are reasonable for sites under consideration.



470 **Declaration of Competing Interests**

471 We declare that we have no financial and personal relationships with other people or  
472 organisations of any kind that could be influencing our work presented in the manuscript titled,  
473 “Two-dimensional vapour intrusion model involving advective transport of vapours with a  
474 highly permeable granular layer in the vadose zone serving as the preferential pathway”.

475 **References**

- 476 2005. Standard Technical Specification for Construction of Sewer Rising Mains. *In:*  
477 CORPORATION, H. W. (ed.).
- 478 ABREU, L. D. & JOHNSON, P. C. 2005. Effect of vapor source– building separation and  
479 building construction on soil vapor intrusion as studied with a three-dimensional  
480 numerical model. *Environmental science & technology*, 39, 4550-4561.
- 481 BECKLEY, L. & MCHUGH, T. 2021. Temporal variability in volatile organic compound  
482 concentrations in sanitary sewers at remediation sites. *Science of The Total  
483 Environment*, 784, 146928.
- 484 CHOI, J.-W., TILLMAN, F. D. & SMITH, J. A. 2002. Relative importance of gas-phase  
485 diffusive and advective trichloroethene (TCE) fluxes in the unsaturated zone under  
486 natural conditions. *Environmental Science & Technology*, 36, 3157-3164.
- 487 DISTLER, M. & MAZIERSKI, P. Soil vapor migration through subsurface utilities. Air &  
488 Waste Management Association, Vapor Intrusion Specialty Conference, 2010.
- 489 EPA, U. 2012. EPA’s Vapor Intrusion Database: Evaluation and Characterization of  
490 Attenuation Factors for Chlorinated Volatile Organic Compounds and Residential  
491 Buildings *In:* RESPONSE, O. O. S. W. A. E. (ed.). Washington, DC.
- 492 GUO, Y., DAHLEN, P. & JOHNSON, P. 2020. Temporal variability of chlorinated volatile  
493 organic compound vapor concentrations in a residential sewer and land drain system  
494 overlying a dilute groundwater plume. *Science of The Total Environment*, 702, 134756.
- 495 GUO, Y., HOLTON, C., LUO, H., DAHLEN, P., GORDER, K., DETTENMAIER, E. &  
496 JOHNSON, P. C. 2015. Identification of alternative vapor intrusion pathways using  
497 controlled pressure testing, soil gas monitoring, and screening model calculations.  
498 *Environmental science & technology*, 49, 13472-13482.
- 499 HOLTON, C., LUO, H., DAHLEN, P., GORDER, K., DETTENMAIER, E. & JOHNSON, P.  
500 C. 2013. Temporal variability of indoor air concentrations under natural conditions in a  
501 house overlying a dilute chlorinated solvent groundwater plume. *Environmental science  
502 & technology*, 47, 13347-13354.
- 503 ITRC 2014. Guidance Document.
- 504 JACOBS, J., JACOBS, O. & PENNELL, K. 2015. One alternate exposure pathway of VOC  
505 vapors from contaminated subsurface environments into indoor air–legacy sewer  
506 plumbing systems. Feature article in the spring 2015 Groundwater Resources  
507 Association of California (GRAC) Newsletter.

508 JOHNSON, P. C. & ETTINGER, R. A. 1991. Heuristic model for predicting the intrusion rate  
509 of contaminant vapors into buildings. *Environmental Science & Technology*, 25, 1445-  
510 1452.

511 MA, J., YAN, G., LI, H. & GUO, S. 2016. Sensitivity and uncertainty analysis for Abreu &  
512 Johnson numerical vapor intrusion model. *Journal of hazardous materials*, 304, 522-  
513 531.

514 MCHUGH, T., BECKLEY, L., SULLIVAN, T., LUTES, C., TRUESDALE, R.,  
515 UPPENCAMP, R., COSKY, B., ZIMMERMAN, J. & SCHUMACHER, B. 2017.  
516 Evidence of a sewer vapor transport pathway at the USEPA vapor intrusion research  
517 duplex. *Science of the Total Environment*, 598, 772-779.

518 MILLINGTON, R. & QUIRK, J. 1961. Permeability of porous solids. *Transactions of the*  
519 *Faraday Society*, 57, 1200-1207.

520 PENNELL, K. G., SCAMMELL, M. K., MCCLEAN, M. D., AMES, J., WELDON, B.,  
521 FRIGUGLIETTI, L., SUUBERG, E. M., SHEN, R., INDEGLIA, P. A. & HEIGER-  
522 BERNAYS, W. J. 2013. Sewer gas: an indoor air source of PCE to consider during  
523 vapor intrusion investigations. *Groundwater Monitoring & Remediation*, 33, 119-126.

524 RIIS, C., CHRISTENSEN, A., HANSEN, M., HUSUM, H. & TERKELSEN, M. Vapor  
525 intrusion through sewer systems: Migration pathways of chlorinated solvents from  
526 groundwater to indoor air. Seventh Battelle International Conference on Remediation  
527 of Chlorinated and Recalcitrant Compounds, Monterey, 2010.

528 ROGHANI, M., JACOBS, O. P., MILLER, A., WILLETT, E. J., JACOBS, J. A., VITERI, C.  
529 R., SHIRAZI, E. & PENNELL, K. G. 2018. Occurrence of chlorinated volatile organic  
530 compounds (VOCs) in a sanitary sewer system: Implications for assessing vapor  
531 intrusion alternative pathways. *Science of The Total Environment*, 616, 1149-1162.

532 SCANLON, B. R., NICOT, J. P. & MASSMANN, J. W. 2002. Soil gas movement in  
533 unsaturated systems. *Soil physics companion*, 389, 297-341.

534 USEPA 2002. OSWER Draft Guidance for Evaluating the Vapor Intrusion to Indoor Air  
535 Pathway from Groundwater and Soils (Subsurface Vapor Intrusion Guidance). *In:*  
536 RESPONSE, O. O. S. W. A. E. (ed.). Washington D.C.: US EPA.

537 USEPA 2015a. OSWER technical guide for assessing and mitigating the vapor intrusion  
538 pathway from subsurface vapor sources to indoor air. *In:* RESPONSE, O. O. S. W. A.  
539 E. (ed.). Washington, DC, USA: OSWER Publication.

540 USEPA 2015b. Technical Guide for Addressing Petroleum Vapor Intrusion at Leaking  
541 Underground Storage Tank Sites. Washington, DC, USA: US Environmental Protection  
542 Agency.

543 VROBLESKY, D. A., PETKEWICH, M. D., LOWERY, M. A. & LANDMEYER, J. E. 2011.  
544 Sewers as a source and sink of chlorinated- solvent groundwater contamination, Marine  
545 Corps Recruit Depot, Parris Island, South Carolina. *Groundwater Monitoring &*  
546 *Remediation*, 31, 63-69.

547 YAO, Y., MAO, F., MA, S., YAO, Y., SUUBERG, E. M. & TANG, X. 2017a. Three-  
548 dimensional simulation of land drains as a preferential pathway for vapor intrusion into  
549 buildings. *Journal of environmental quality*, 46, 1424-1433.

550 YAO, Y., PENNELL, K. G. & SUUBERG, E. M. 2012. Estimation of contaminant subslab  
551 concentration in vapor intrusion. *Journal of hazardous materials*, 231, 10-17.

552 YAO, Y., SHEN, R., PENNELL, K. G. & SUUBERG, E. M. 2013. Estimation of contaminant  
553 subslab concentration in vapor intrusion including lateral source–building separation.  
554 *Vadose Zone Journal*, 12.

555 YAO, Y., VERGINELLI, I. & SUUBERG, E. M. 2017b. A two-dimensional analytical model  
556 of vapor intrusion involving vertical heterogeneity. *Water Resour Res*, 53, 4499-4513.

557 YAO, Y., WU, Y., WANG, Y., VERGINELLI, I., ZENG, T., SUUBERG, E. M., JIANG, L.,  
558 WEN, Y. & MA, J. 2015. A petroleum vapor intrusion model involving upward  
559 advective soil gas flow due to methane generation. *Environmental science &*  
560 *technology*, 49, 11577-11585.

561

562

## LIST OF TABLES

**Table 1. Input parameters for the model simulations.**

<i>Chemical Parameters</i>		<i>Unit</i>	<i>Value</i>
<i>Source vapour concentration</i>	$C_s$	g/m <sup>3</sup>	1
<i>Diffusion coefficient in air</i>	$D_a$	m <sup>2</sup> /s	7.90E-06
<i>Diffusion coefficient in water</i>	$D_w$	m <sup>2</sup> /s	9.10E-10
<i>Henry's law constant</i>	$H$	-	0.403
<i>Soil gas viscosity</i>	$\mu$	Pa.s	5.32E-04
<b><i>Soil Parameters</i></b>			
<i>Total Porosity</i>	$\Theta_T$	-	0.385
<i>Air filled porosity</i>	$\Theta_a$	-	0.188
<i>Water filled porosity</i>	$\Theta_w$	-	0.197
<i>Soil air permeability</i>	$K_a$	m <sup>2</sup>	1.70E-13
<b><i>Granular backfill soil parameters</i></b>			
<i>Depth of backfill</i>	$d_s$	m	0.5
<i>Total Porosity</i>	$\Theta_T$	-	0.5
<i>Air filled porosity</i>	$\Theta_a$	-	0.49
<i>Water filled porosity</i>	$\Theta_w$	-	0.01
<i>Soil air permeability</i>	$K_a$	m <sup>2</sup>	1.00E-09
<b><i>Building parameters</i></b>			
<i>Width of foundation slab</i>		m	10
<i>Foundation footprint area</i>	$A_b$	m <sup>2</sup>	100
<i>Depth of foundation below grade</i>	$d_f$	m	0.3
<i>Thickness of foundation crack</i>	$t_{ck}$	m	0.1
<i>Width of foundation crack</i>	$w_{ck}$	m	0.001
<i>Foundation perimeter</i>	$l_{ck}$	m	40
<i>Building height</i>	$L_{mix}$	m	3
<i>Building Air exchange rate</i>	$ER$	h <sup>-1</sup>	0.5
<i>Soil and building pressure difference</i>	$\Delta p$	Pa	5

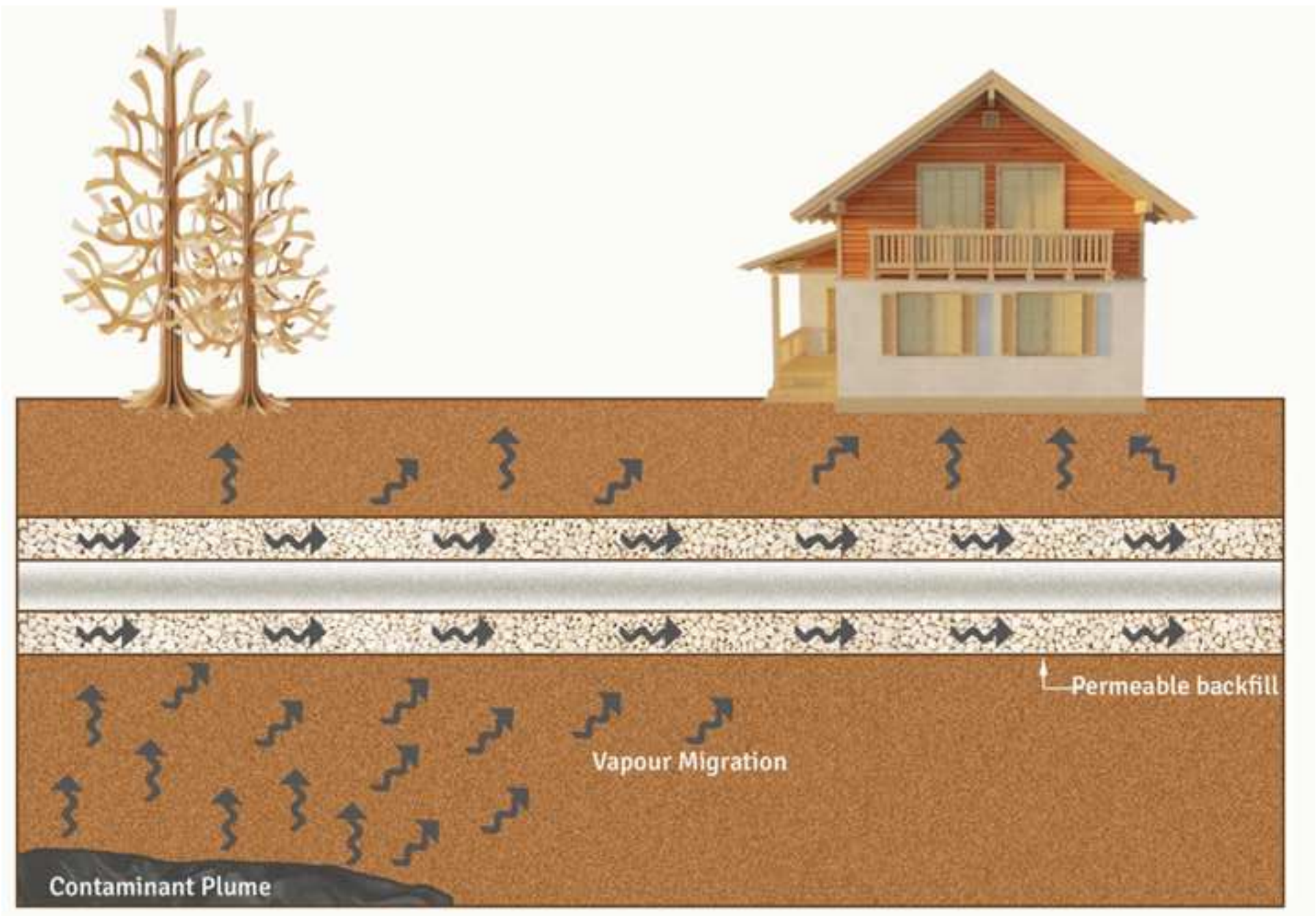
**Table 2. Comparison of sub-slab concentration, indoor air concentration and attenuation factor with and without the preferential pathway for different scenarios.**

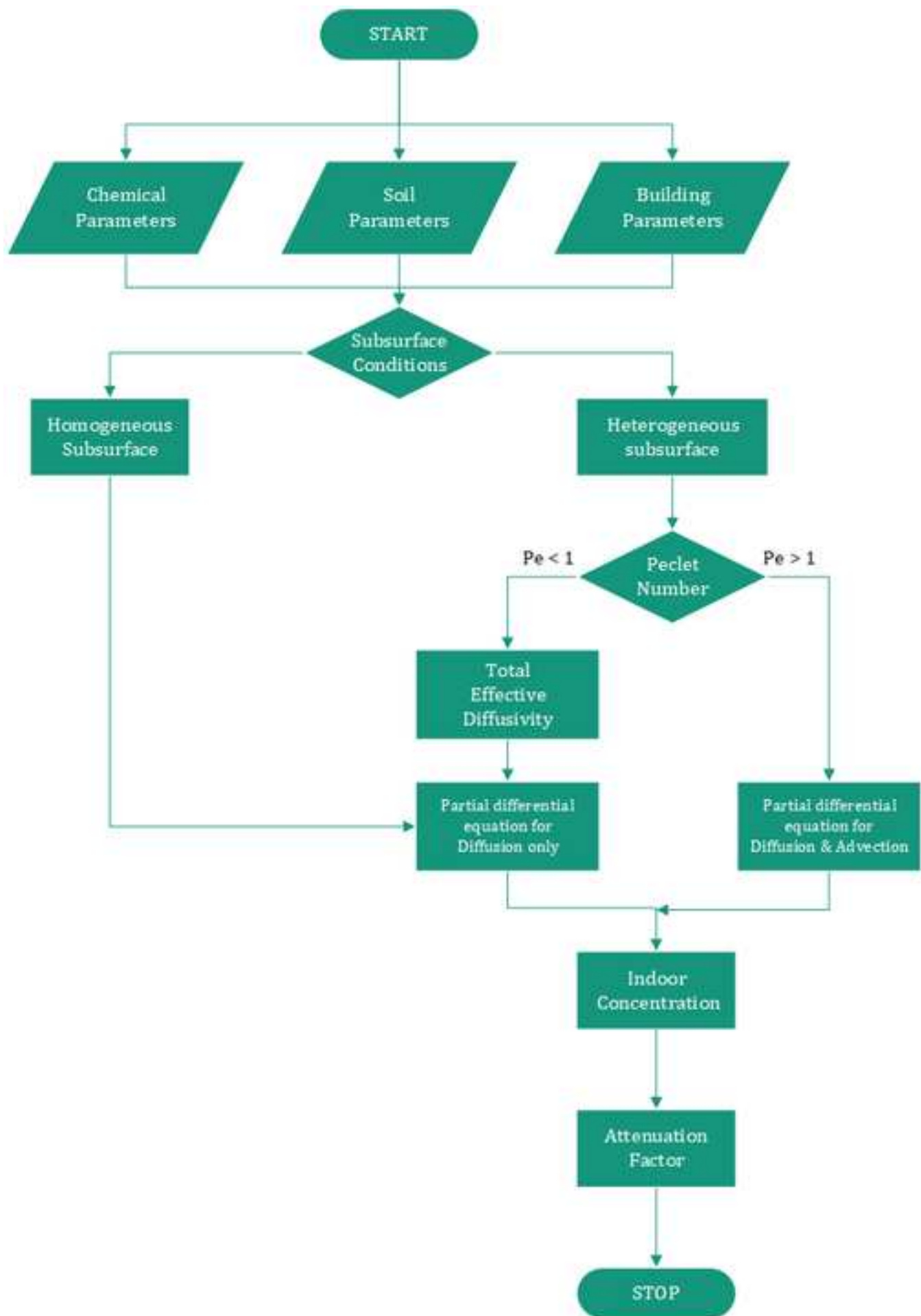
	<i>Without preferential pathway</i>	<i>With preferential pathway</i>
<i>Source concentration (g/m<sup>3</sup>)</i>	1	1
<i>Sub-slab concentration (g/m<sup>3</sup>)</i>	0.025	0.048
<i>Indoor air concentration (g/m<sup>3</sup>)</i>	3.86E-05	7.40E-05
<i>Attenuation factor (<math>\alpha</math>)</i>	3.86E-05	7.40E-05

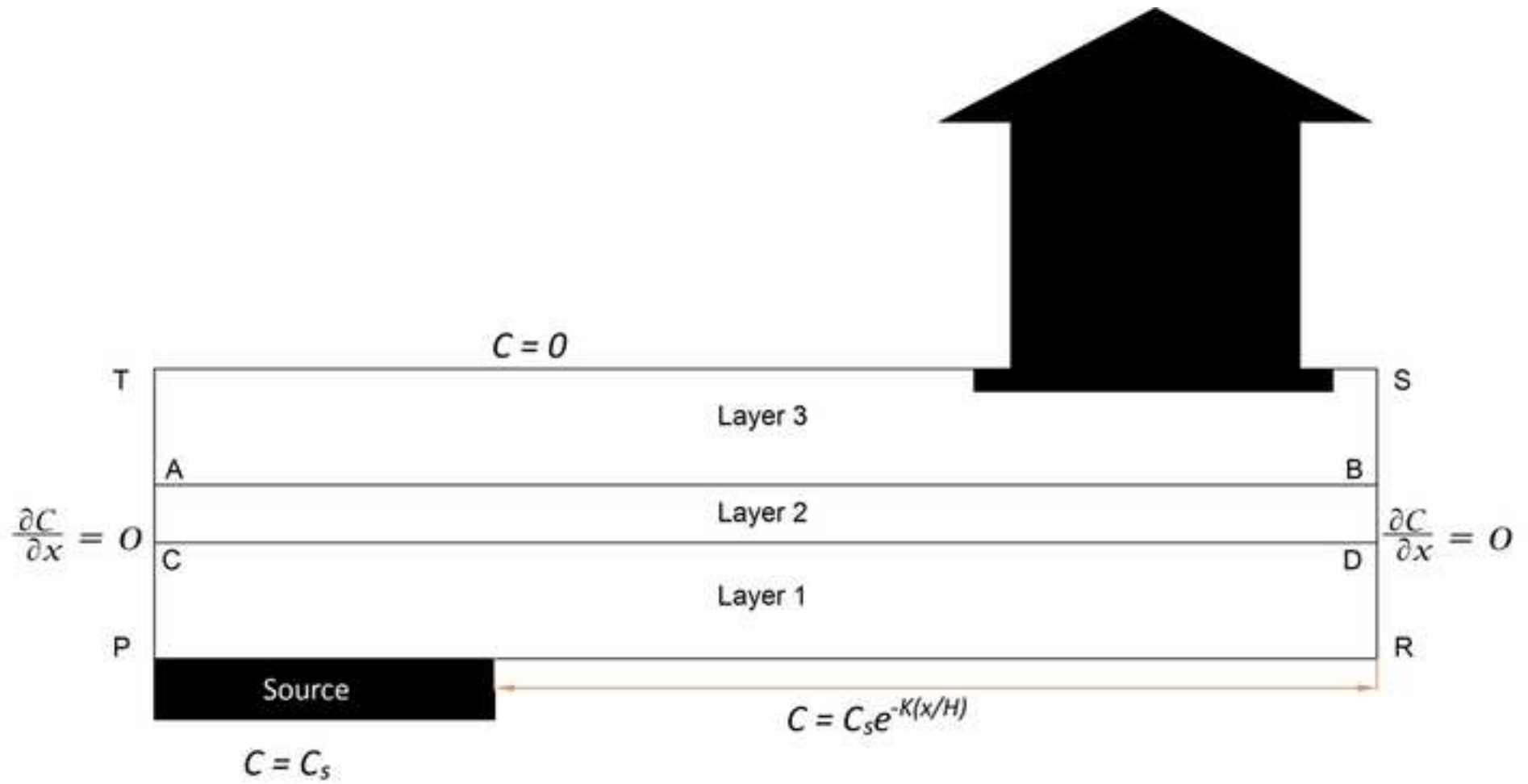
**Table 3. Soil characteristics for 12 typical soils summarised in US EPA database**

<i>Soil Type</i>	<i>Total Porosity</i>	<i>Water-filled porosity</i>	<i>Soil permeability (m<sup>2</sup>)</i>
<i>Clay</i>	0.459	0.215	2.32x10 <sup>-13</sup>
<i>Clay Loam</i>	0.442	0.168	1.29x10 <sup>-13</sup>
<i>Loam</i>	0.399	0.148	1.90x10 <sup>-13</sup>
<i>Loamy sand</i>	0.390	0.076	1.67x10 <sup>-12</sup>
<i>Sand</i>	0.375	0.054	1.02x10 <sup>-11</sup>
<i>Sandy clay</i>	0.385	0.197	1.79x10 <sup>-13</sup>
<i>Sandy clay loam</i>	0.384	0.146	2.09x10 <sup>-13</sup>
<i>Sandy loam</i>	0.387	0.103	6.09x10 <sup>-13</sup>
<i>Silt</i>	0.489	0.167	6.92x10 <sup>-13</sup>
<i>Silt loam</i>	0.439	0.180	2.89x10 <sup>-13</sup>
<i>Silty clay</i>	0.481	0.216	1.52x10 <sup>-13</sup>
<i>Silty clay loam</i>	0.482	0.198	1.75x10 <sup>-13</sup>

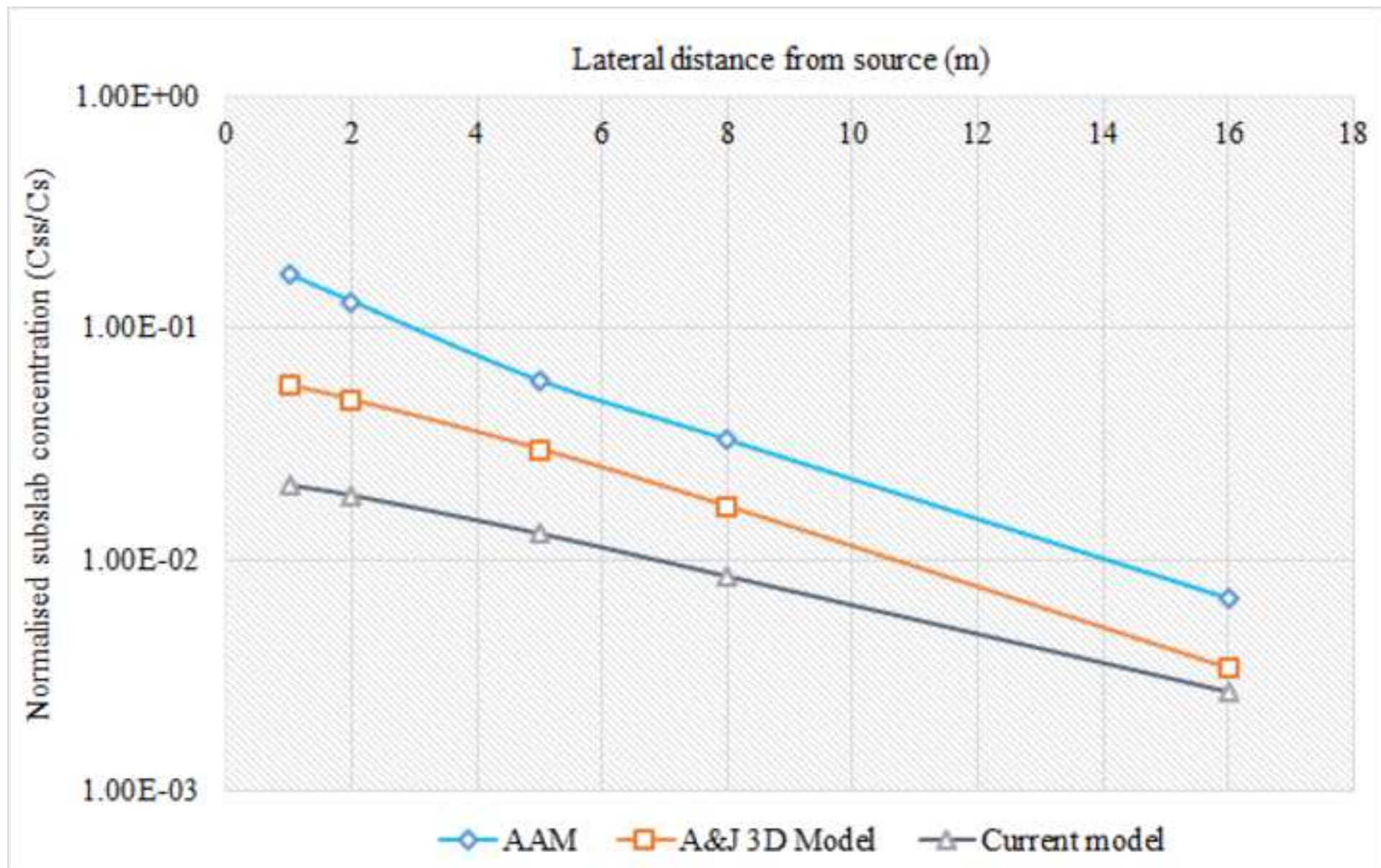
Figure 1

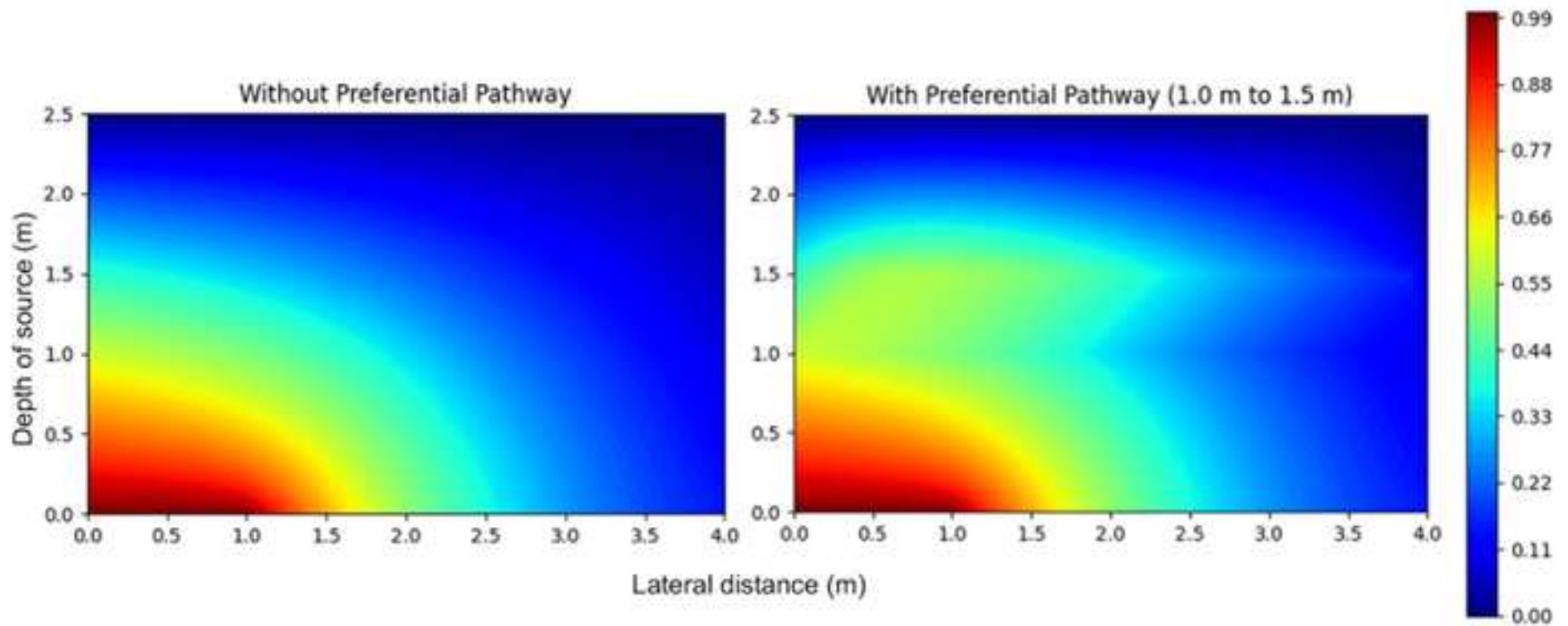


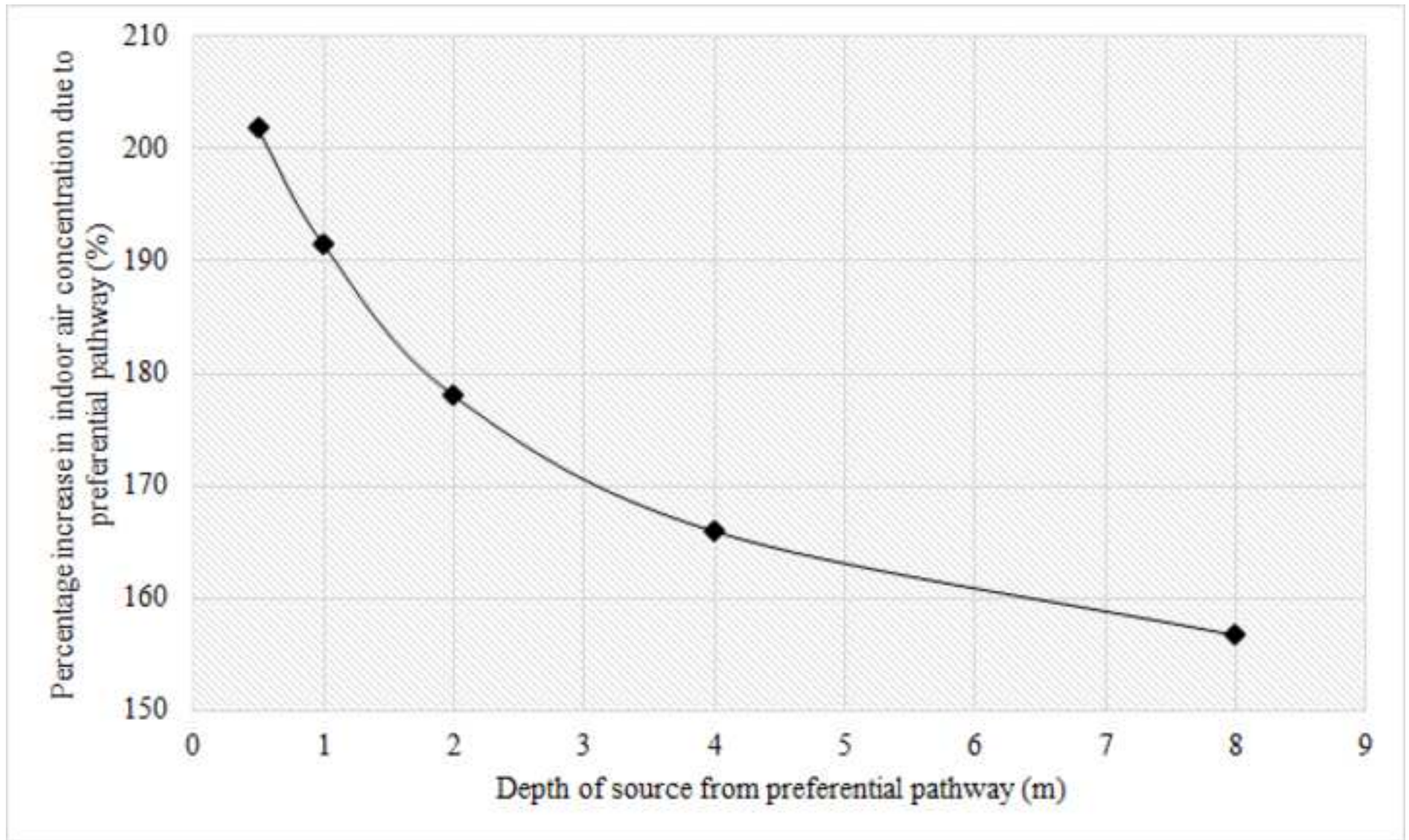


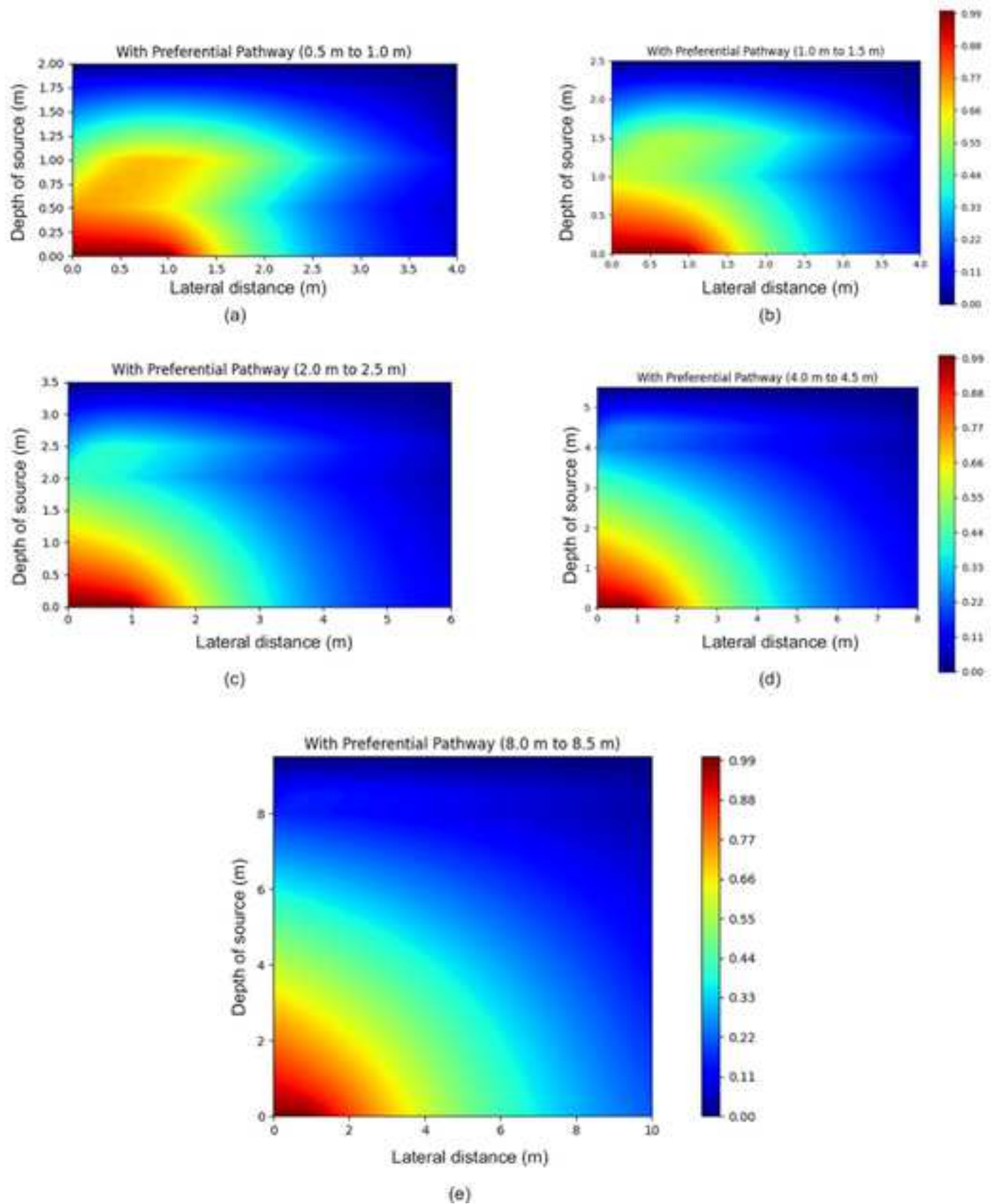


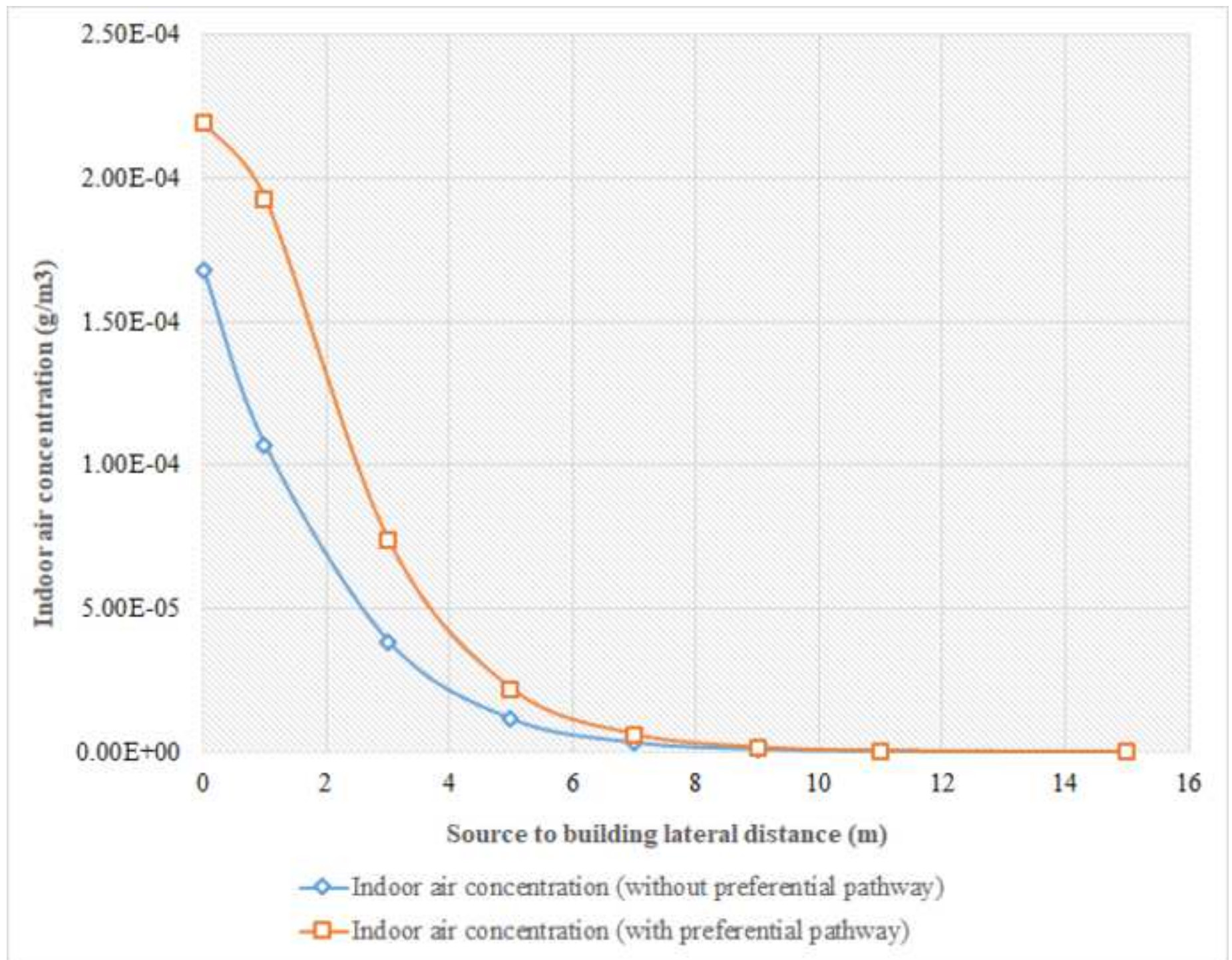


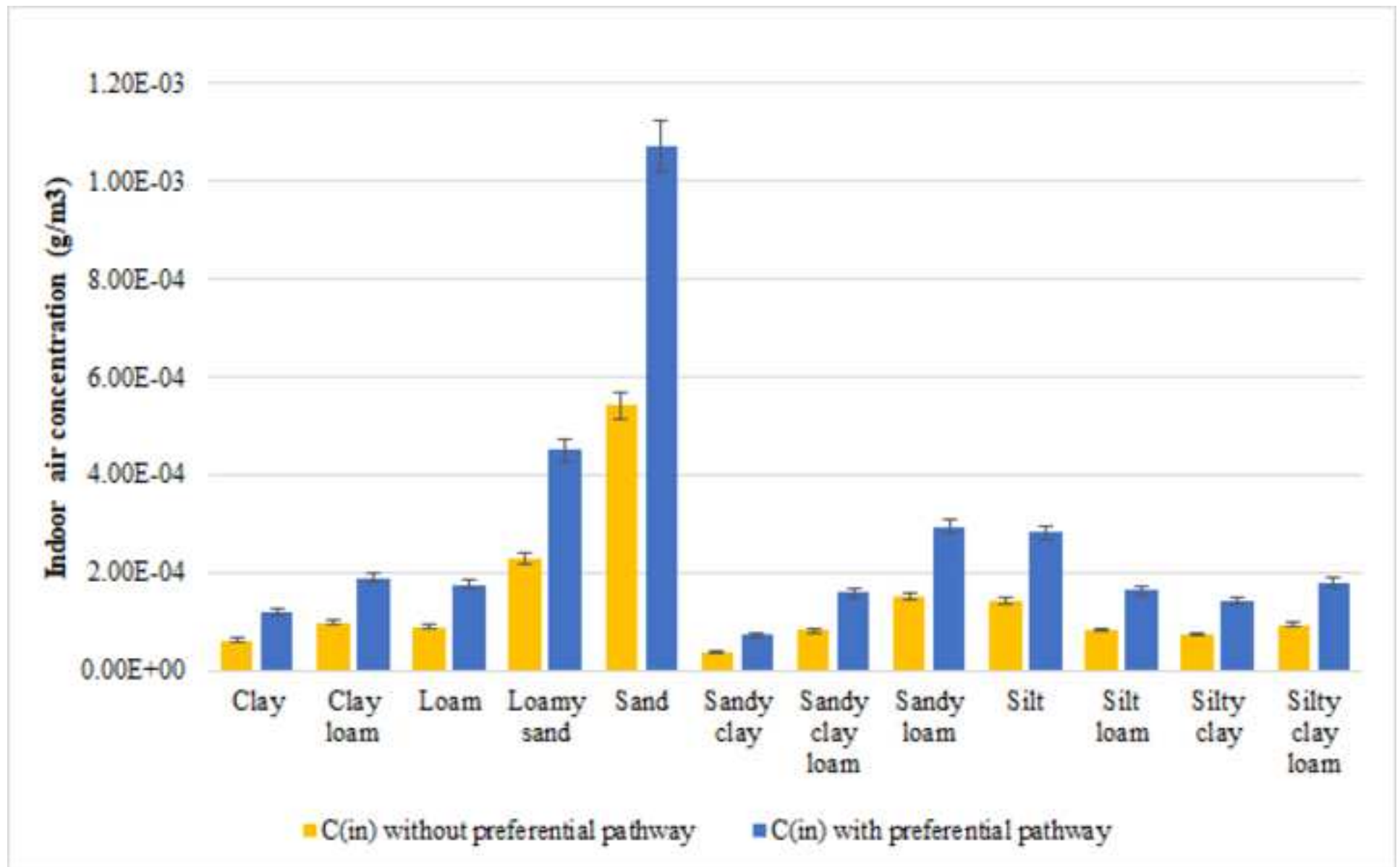




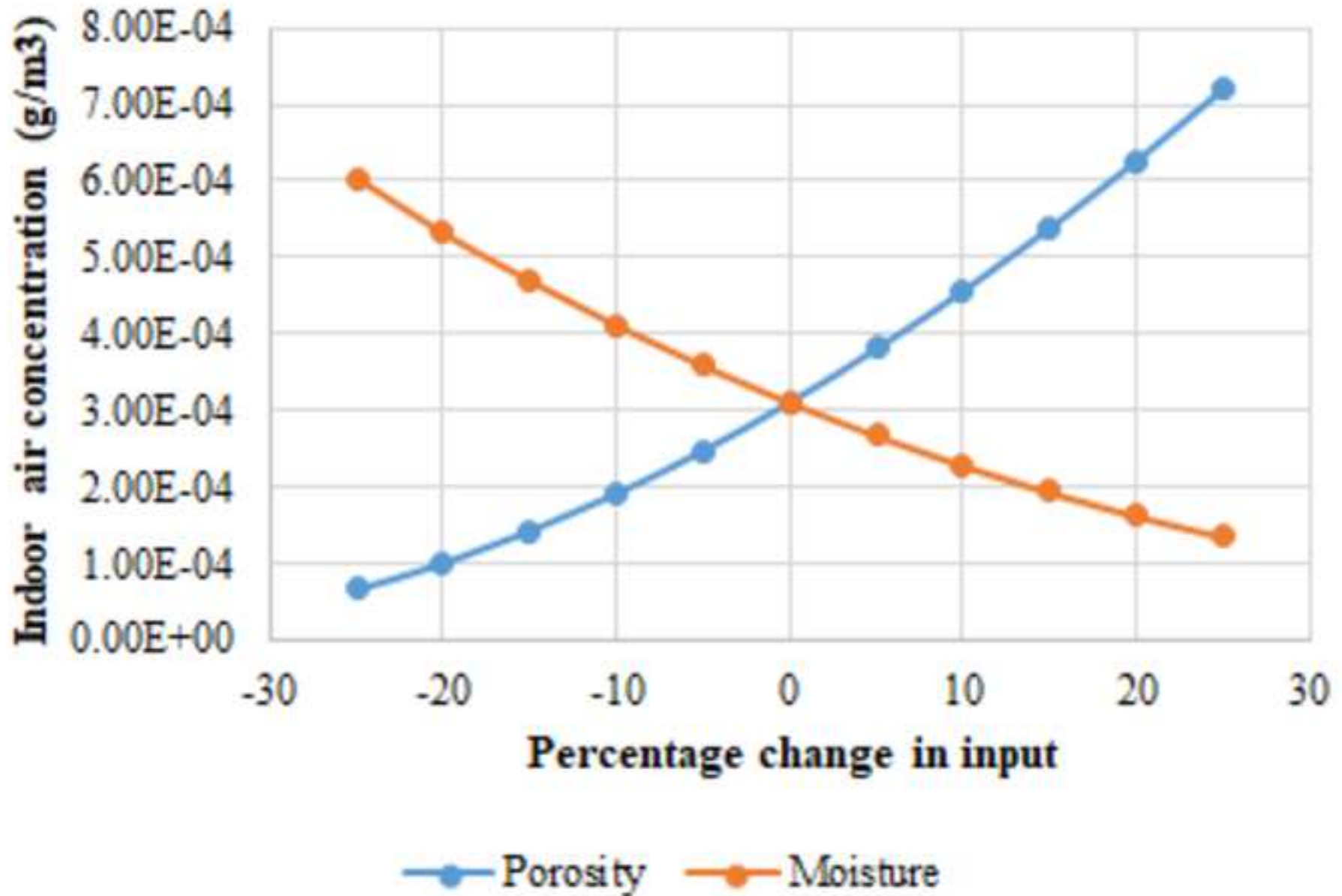


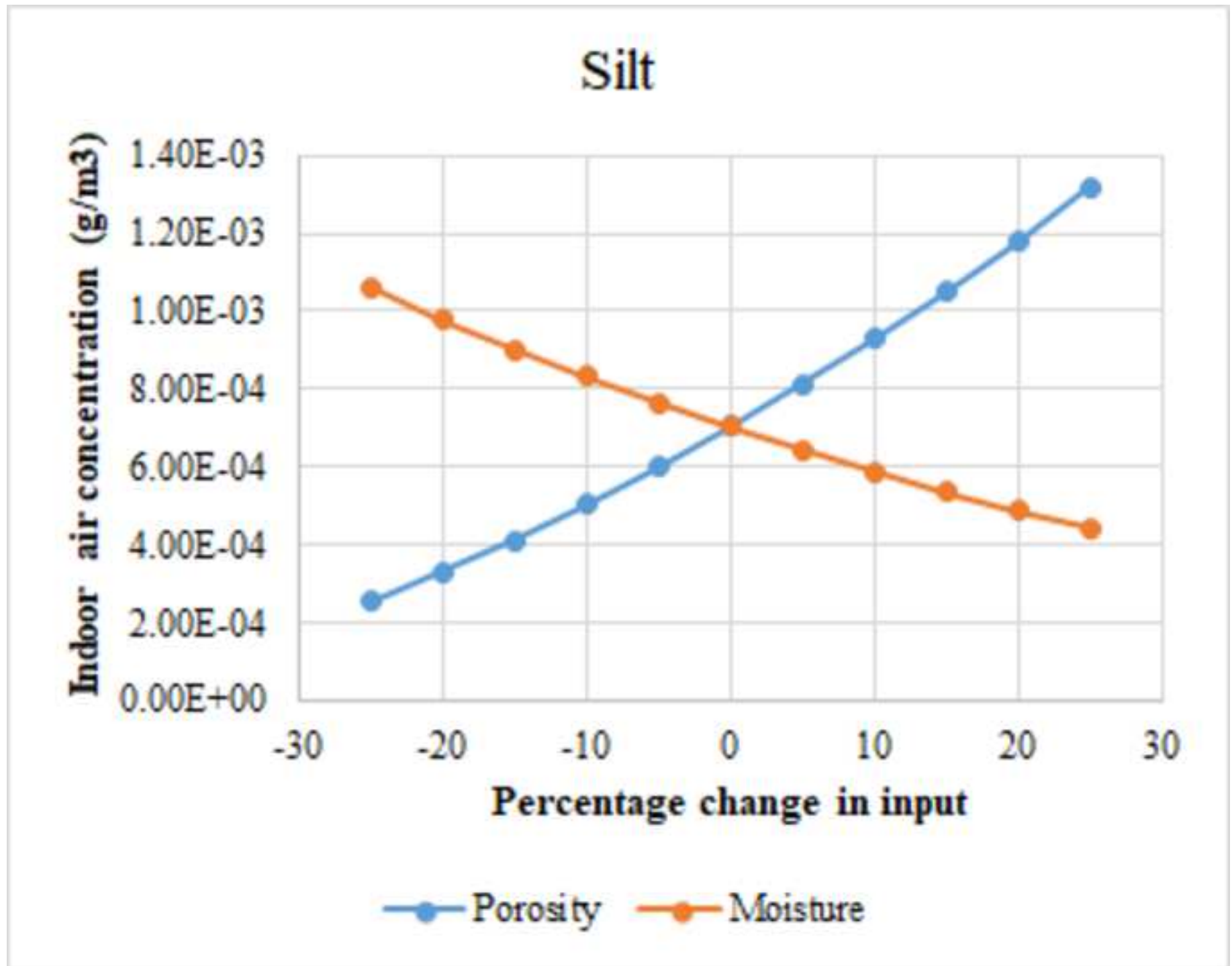




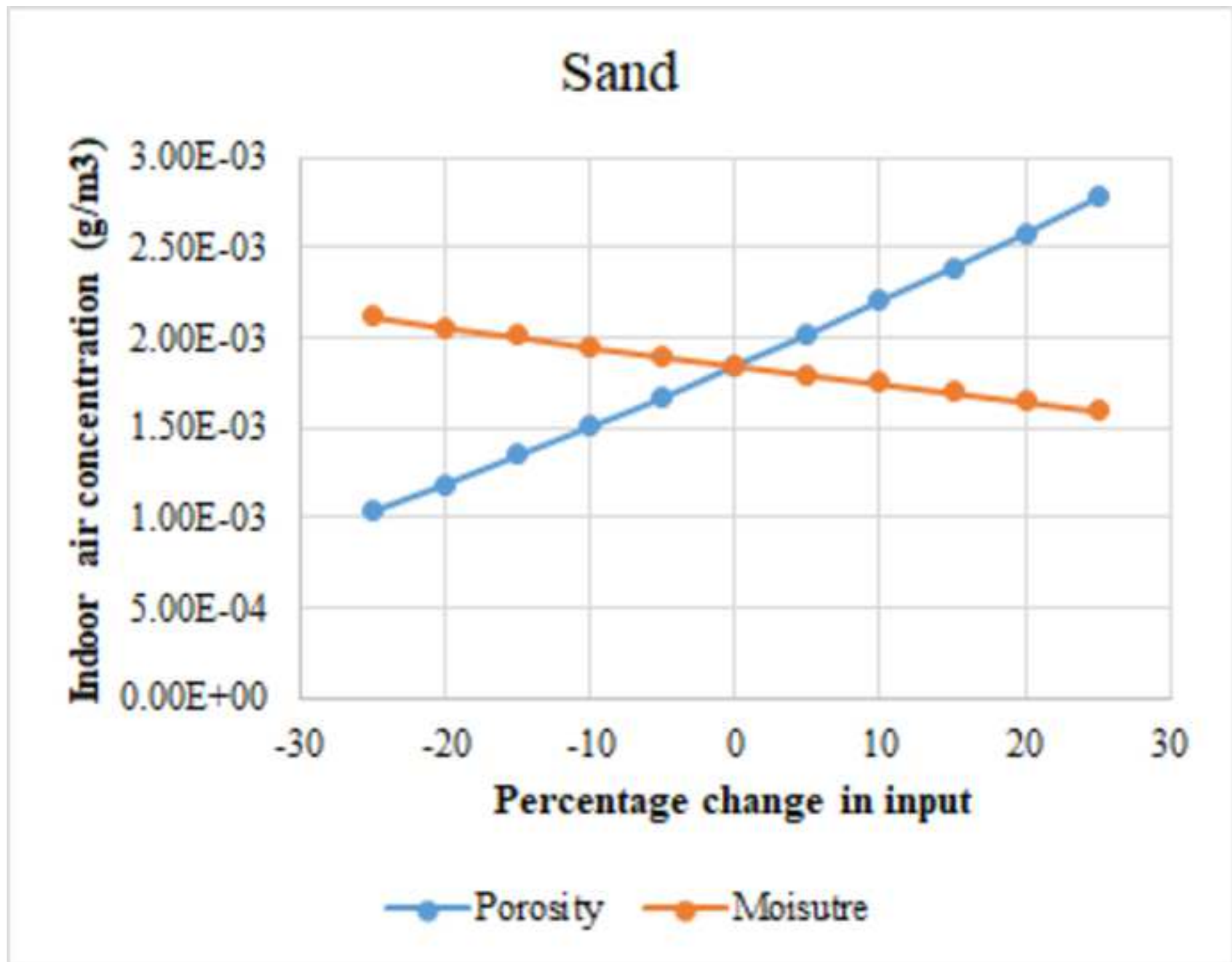


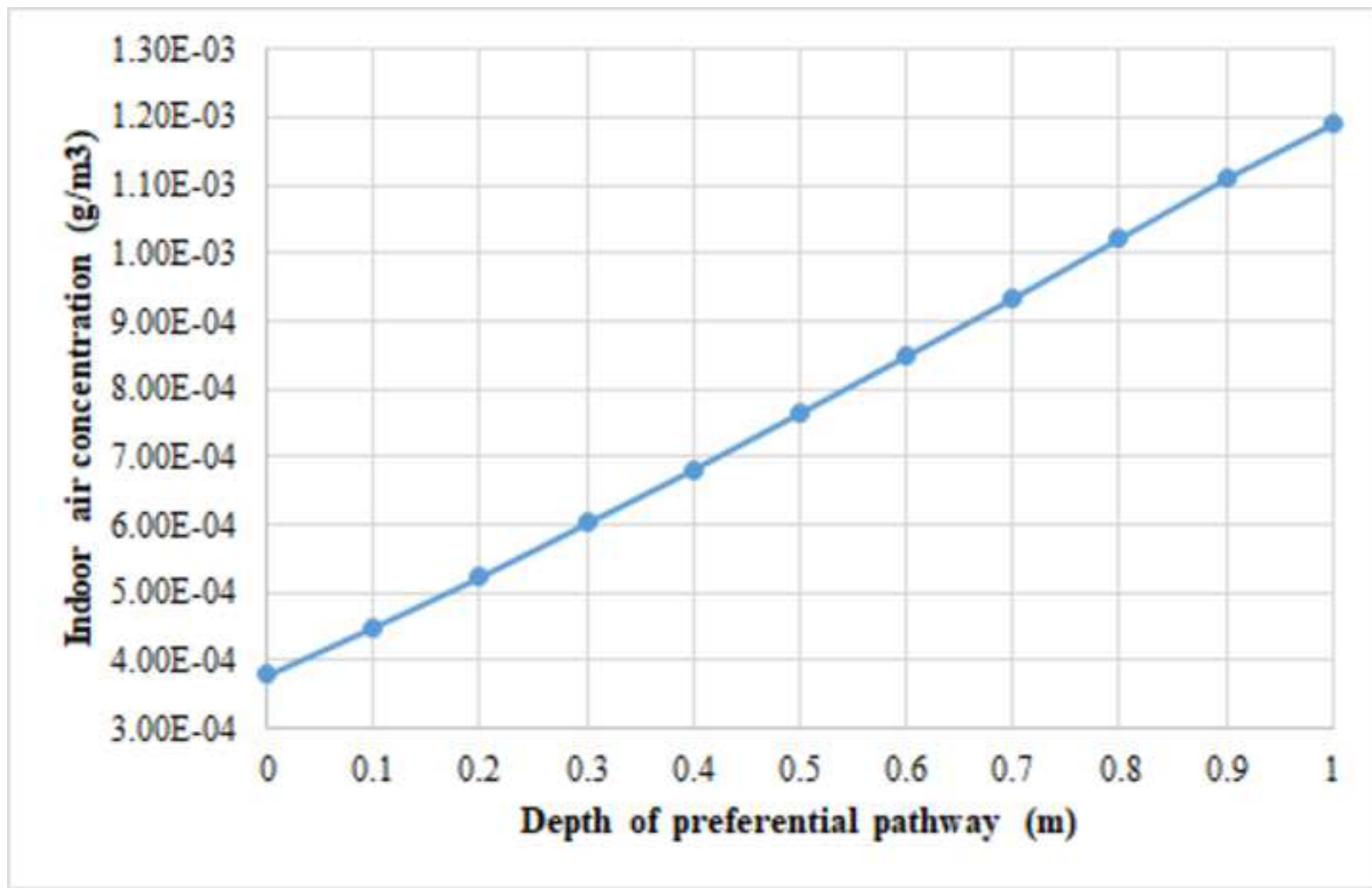
# Clay











**Declaration of interests**

The authors declare that they have no known competing financial interests or personal relationships that could have appeared to influence the work reported in this paper.

The authors declare the following financial interests/personal relationships which may be considered as potential competing interests:

### **CRedit author statement**

Aravind Unnithan, Methodology, Investigation, Formal analysis, Writing - Original Draft;  
Dawit Nega Bekele, Methodology, Formal analysis, Supervision, Writing - Review &  
Editing; Sreenivasulu Chadalavada, Methodology, Supervision, Resources, Writing - Review  
& Editing; Ravi Naidu, Conceptualization, Writing - Review & Editing, Supervision,  
Funding acquisition;